Research Square

Preprints are preliminary reports that have not undergone peer review.
They should not be considered conclusive, used to inform clinical practice,
or referenced by the media as validated information.

The hijacking of a wheat Exo70-like protein by a fungal pathogen triggers disease

Justin Faris

justin.faris@usda.gov

United States Department of Agriculture-Agricultural Research Service, Cereal Crops Research Unit, Edward T. Schafer Agricultural Research Center, Fargo, North Dakota 58102, USA
https://orcid.org/0000-0002-9653-3287

Gurminder Singh
https://orcid.org/0000-0002-2637-7282

Katherine Running
North Dakota State University

Sudeshi Seneviratne
North Dakota State University

Krishna Acharya
North Dakota State University https://orcid.org/0000-0003-0538-1028

Tiana Roth
North Dakota State University

Amanda Peters Haugrud
USDA-ARS Edward T. Shafer Agricultural Research Center

Zengcui Zhang
USDA-ARS Edward T. Shafer Agricultural Research Center

Agnes Szabo-Hever
North Dakota State University

Pooja Kumari
North Dakota State University

Phillip McClean
North Dakota State U https://orcid.org/0000-0002-4809-0864

Zhaohui Liu
North Dakota State University https://orcid.org/0000-0002-8106-9186

Shengming Yang
Edward T. Schafer Agricultural Research Center, USDA-ARS

Article

Keywords:

Posted Date: February 9th, 2026

DOI: https://doi.org/10.21203/rs.3.rs-8788414/v1

License: This work is licensed under a Creative Commons Attribution 4.0 International License.
Read Full License

Additional Declarations: There is **NO** Competing Interest.

Version of Record: A version of this preprint was published at Nature Communications on September 10th, 2026. See the published version at https://doi.org/10.1038/s41467-026-77720-9.

The hijacking of a wheat *Exo70*-like protein by a fungal pathogen triggers disease

Gurminder Singh[1,3], Katherine L.D. Running[1], Sudeshi Seneviratne[1], Krishna Acharya[1], Tiana M. Roth[1], Amanda R. Peters Haugrud[2], Zengcui Zhang[2], Agnes Szabo-Hever[1], Pooja Kumari[1], Phillip E. McClean[1], Zhaohui Liu[3], Shenming Yang[2], and Justin D. Faris[2*]

[1]Department of Plant Sciences, North Dakota State University, Fargo, ND, USA

[2]USDA-ARS, Edward T. Schafer Agricultural Research Center, Fargo, ND, USA

[3]Department of Plant Pathology, North Dakota State University, Fargo, ND, USA

*Corresponding author: justin.faris@usda.gov

Abstract

Tan spot is an economically important fungal disease of wheat that occurs globally. In this necrotrophic pathosystem, pathogen effectors are recognized by wheat genes in an inverse gene-for-gene manner, leading to the hijacking of host defense mechanisms and ultimately disease susceptibility. Here, we identified the tan spot susceptibility gene *Tsc2* through positional cloning, mutagenesis, and transgenic complementation. *Tsc2* encodes a diverged form of the exocyst subunit Exo70FX15 that localizes to the nucleus and cytoplasm and does not interact directly with the fungal effector. A 21-nucleotide deletion in *Tsc2* occurred in durum wheat more than a century ago and subsequently spread to common wheat through breeding practices, which allowed recognition of the pathogen effector and subsequent hijacking of the host immune system. We demonstrate that elimination of *Tsc2* through conventional breeding using a diagnostic marker or disruption of *Tsc2* by gene editing can be used to improve tan spot resistance in wheat.

Introduction

Wheat (*Triticum* spp.) is cultivated on more than 215 million hectares and supplies nearly 20% of the calories and protein in the human diet worldwide[1]. As global demand for wheat continues to rise, safeguarding its productivity has become a critical priority for food security[2]. Yet several foliar diseases continue to erode attainable yields. Among these, tan spot (also known as yellow spot), caused by the necrotrophic fungus *Pyrenophora tritici-repentis* (Ptr), has emerged as a globally pervasive and damaging foliar disease of common (bread) wheat (*T. aestivum* L., $2n = 6x = 42$, AABBDD genomes) and durum (pasta) wheat (*T. turgidum* L. ssp. *durum* (Desf.) van Slageren, $2n = 4x = 28$, AABB genomes) that compromises both grain yield and quality[3–5]. Recent global burden analyses rank tan spot among the six most damaging wheat diseases[6], costing growers hundreds of millions of dollars and resulting in losses of nearly 22.4 billion loaves of bread annually[7]. Meta-analyses estimate average yield losses of 5-10%, with documented epidemic losses of up to 50% under conducive conditions[6,8–11]. The rapid expansion of conservation tillage that began in the 1970s has intensified disease pressure by allowing Ptr to overwinter on infected crop residue, and warming weather patterns are expected to extend the pathogen's geographic range[5,12,13].

Current management of tan spot relies on agronomic practices such as crop rotation, residue management, and timely fungicide applications to reduce inoculum and suppress disease development[14–16]. However, these approaches are constrained by agronomic feasibility, economic cost, and environmental sustainability. Genetic resistance offers the most durable and environmentally sound solution, but breeding progress has been hampered by the distinctive pathogenic strategy of Ptr[5].

Biotrophs such as the rust and mildew pathogens require living tissue to acquire nutrients and are typically thwarted when classical resistance (R) genes trigger programmed cell death (PCD) and associated defense responses. But contrary to biotrophic pathogens, necrotrophic pathogens require dead or dying cells to acquire nutrients. To achieve this, Ptr employs necrotrophic effectors (NEs) that act to hijack the plant's immune system through recognition by specific host genes that activate PCD and the 'defense response'[5,17]. Therefore, the lifestyles of necrotrophs such as Ptr have made it possible for them to obtain the ability to exploit the innate immune systems of plants for their own benefit.

Three Ptr-produced NEs named Ptr ToxA, Ptr ToxB, and Ptr ToxC have been characterized[18–20]. These NEs rely on recognition by the dominant host genes *Tsn1*, *Tsc2*, and *Tsc1*, respectively, to trigger susceptibility[5]. This inverse gene-for-gene system has become a foundational model for understanding necrotrophic plant-pathogen interactions[21].

The tan spot susceptibility genes *Tsn1* and *Tsc1* have been cloned and functionally characterized. *Tsn1* encodes a protein with integrated serine/threonine protein kinase (PK), nucleotide-binding, and leucine-rich repeat (NLR) domains[17]. *Tsc1* encodes a membrane-spanning leucine-rich repeat receptor-like kinase (LRR-RLK)[22,23]. The identification and characterization of *Tsn1* and *Tsc1* have demonstrated that Ptr can subvert immune-receptor architecture involving both effector- and pathogen-associated molecular pattern (PAMP)-triggered immunity (ETI and PTI) pathways to drive host cell death[21].

The role of a compatible *Tsc2*-Ptr ToxB interaction in tan spot development has been well established in both common wheat[24–27] and durum wheat[28–30]. Ptr ToxB is a 6.5-kDa, cysteine-rich secreted effector encoded by a gene that exists in multiple tandem copies on a mobile 294-kb "Starship" element[31]. Population surveys revealed that this locus undergoes

frequent duplication, loss, and diversifying selection, shaping virulence diversity worldwide[32,33]. Fluorescent tagging, apoplastic fluid extractions, and heterologous expression experiments demonstrated that Ptr ToxB remains extracellular, and it alone is sufficient to induce chlorosis in the presence of *Tsc2*, indicating that it acts in the leaf apoplast rather than entering host cells[34,35]. Previous linkage studies placed *Tsc2* on wheat chromosome arm 2BS and delimited it to a 1.9 Mb region, but the causal gene has not been identified[24,26,27,30].

Here, we show that *Tsc2* encodes a previously uncharacterized member of the exocyst subunit Exo70 family that is necessary and sufficient to confer Ptr ToxB-triggered cell death. Natural or induced loss-of-function alleles abolish effector sensitivity and confer resistance to tan spot. A 21-nucleotide (nt) deletion in *Tsc2* that likely occurred in a domesticated durum wheat variety and subsequently spread to hexaploid common wheat through breeding practices is required for Ptr ToxB recognition and the subsequent hijacking of defense mechanisms. Together, these findings deepen our understanding of functionalization of *Exo70*-like genes in host-pathogen interactions and necrotrophic disease susceptibility while delivering practical tools such as diagnostic markers and gene editing methods to support the development of more resilient cultivars.

Results

Tsc2 mapping and candidate gene identification

The *PtrToxB* gene was cloned into a yeast expression vector of *Pichia pastoris* as described previously[36], and cultures of the recombinant *P. pastoris* expressing the Ptr ToxB protein were infiltrated into wheat leaves to determine if plants were sensitive or insensitive as a proxy for Ptr ToxB-induced disease[30,34] (Fig. 1). Plants that display cell death in the form of

chlorosis carry the dominant *Tsc2* allele, whereas those showing no reaction have a recessive or absent allele[5]. A tetraploid wheat mapping population of 149 recombinant inbred lines (RILs) derived from a cross between the durum cultivars Kronos (Ptr ToxB-sensitive) and Gredho (Ptr-ToxB insensitive) (KG RIL population) was genotyped with the Illumina iSelect 90K SNP array (Supplementary Table 1) and infiltrated with Ptr ToxB cultures (Supplementary Table 2). Genetic linkage analysis delineated the *Tsc2* locus to a 5.6 cM interval on the short arm of chromosome 2B (Fig. 2A), consistent with its previously reported position[24,26,27,30].

To saturate the *Tsc2* region between SNP markers *IWB227* and *IWA2407*, we developed 43 additional simple sequence repeat (SSR) and Kompetitive allele-specific PCR (KASP) markers (*fcp1022* to *fcp1064*) based on the intervening genome sequence in Kronos[37] (Fig. 2B, Supplementary Table 3). In the revised chromosome 2B genetic map, these markers further delineated the *Tsc2* locus to 1.1 cM.

To further refine the region, 7,002 F_2 plants from Kronos × Gredho were infiltrated with Ptr ToxB, and 1,492 insensitive plants (homozygous recessive for *Tsc2*) were used for high-resolution mapping. Among these, 159 plants with recombination events between markers *fcp1023* and *fcp1062* were identified. Genotyping of these recombinants further delimited *Tsc2* to a 0.1 cM interval flanked by markers *fcp1028* and *fcp1033* (Fig. 2C). Alignment with the Kronos genome assembly[37] placed this segment at 30.240-30.349 Mb on chromosome 2B, a span of 108.4 kb harboring six predicted gene models (Fig. 2D, Supplementary Table 4).

The gene content of the 108.4 kb interval was examined in 12 wheat lines with available sequenced genomes, which included four Ptr ToxB-sensitive lines and eight insensitive lines (Supplementary Table 5). Four of the six genes were conserved across all 12 lines, whereas two genes displayed polymorphisms between sensitive and insensitive lines and were considered

120 *Tsc2* candidates. One candidate gene, *TrturKRN2B01G009130*, encoded an LRR-RLK and was
121 intact in the genomes of the four Ptr ToxB-sensitive lines, but it was either absent or carried
122 nonsynonymous SNPs in the insensitive lines. The second candidate gene,
123 *TrturKRN2B01G009140* (Fig. 2E), encoded an unconventional Exo70 subunit (hereafter referred
124 to as *TtExo70FX15*). This gene was 100% identical in all Ptr ToxB-sensitive lines, and it was
125 either absent or lacking a 21-nt in-frame deletion in all insensitive lines.
126
127 **Validation of *Tsc2* candidates by loss-of-function mutants**
128 To determine if either candidate gene was necessary for Ptr ToxB-sensitivity, we
129 evaluated Kronos Targeting Local Lesions IN Genomes (TILLING) lines[38] that carried nonsense
130 or predicted deleterious missense mutations in either the LRR-RLK gene
131 (*TrturKRN2B01G009130*) or *TtExo70FX15*. Of 19 independent TILLING lines with mutations
132 in the LRR-RLK gene, all plants exhibited cell death following infiltration, the same as wild-type
133 Kronos, demonstrating that *TrturKRN2B01G009130* was not necessary for Ptr ToxB-sensitivity
134 (Supplementary Table 6).
135 Ten Kronos TILLING lines with nonsense or missense mutations in *TtExo70FX15* were
136 examined (Supplementary Table 7). Among those, four with nonsense mutations (W149*,
137 W301*, W391*, and Q395*) and five with missense mutations (E125V, A175T, A186T,
138 V187M, and G500E) were insensitive to Ptr ToxB (Fig. 3, Supplementary Figure 1). One
139 missense variant (H393Y) in TILLING line Kronos3105 with tolerated SIFT scores and neutral
140 Missense-3D predictions retained sensitivity. The retention of sensitivity in the H393Y mutant
141 may reflect its predicted stabilizing effect (Dynamut2 $\Delta\Delta G$ = +1.13 kcal/mol), which could
142 maintain native protein conformation and function.

Independent corroboration came by conducting a forward genetic screen of 1,050 ethyl methanesulfonate (EMS)-treated M_2 families of the Ptr ToxB-sensitive hexaploid wheat cultivar Prosper. Fifteen insensitive M_2 families were recovered, and comparative sequence analysis revealed that each family carried a nonsense or missense mutation in the Prosper copy of *TtExo70FX15* (Supplementary Table 7, Fig. 3, Supplementary Figure 2). Taken together, every protein-truncating mutation and all but one missense mutation (Kronos3105) in *TtExo70FX15* converted Ptr ToxB-sensitive wheat to an insensitive state. In contrast, none of mutations in the LRR-RLK gene (*TrturKRN2B01G009130*) affected Ptr ToxB sensitivity. These results confirmed that *TtExo70FX15* is necessary for Ptr ToxB-sensitivity, and together with the results of genetic linkage analysis, provided strong evidence that it was *Tsc2*.

Transgenic complementation confirms *TtExo70FX15* as *Tsc2*

To determine whether *TtExo70FX15* is sufficient to confer sensitivity to Ptr ToxB, a 6.5-kb genomic fragment comprising the Kronos *TtExo70FX15* coding sequence plus its native promoter and terminator was introduced into the Ptr ToxB-insensitive hexaploid spring wheat cultivar Fielder. A single T_0 transformant was verified by gene-specific PCR and Sanger sequencing. Infiltration of leaves with Ptr ToxB revealed that all transgene-positive tillers were as sensitive as Kronos (Fig. 4). In contrast, wild-type Fielder and Gredho controls remained symptom-free. The gain-of-function phenotype in Fielder, together with loss-of-function insensitivity in nine independent Kronos TILLING lines and 15 independent Prosper EMS lines, demonstrated that *TtExo70FX15* was both necessary and sufficient for Ptr ToxB-induced cell death. Therefore, *TtExo70FX15* was demonstrated to be the causal gene functioning as *Tsc2,* and it will hereafter be referred to as the latter.

166

167 ***Tsc2* characterization and transcriptional expression**

168 cDNA sequencing revealed *Tsc2* is an intronless gene of 1,503 bp (Fig. 2E) that encodes
169 a 500-amino-acid protein. The sizes of the untranslated regions (UTRs) were variable, with the 5′
170 UTR ranging from 13 to 153 bp and the 3′ UTR from 132 to 244 bp, but sizes of 19 and 145 bp
171 occurred most frequently for the 5′ and 3′ UTRs, respectively. Reverse transcription (RT)-PCR
172 detected abundant *Tsc2* transcripts in leaf and stem tissues, but comparatively less in root and
173 immature spike tissue (Fig. 5).

174 To determine whether *Tsc2* transcription is modulated by Ptr ToxB, leaves of two-week-
175 old Kronos plants were infiltrated with Ptr ToxB culture, or with a control culture media [yeast-
176 peptone-dextrose (YPD)] not producing Ptr ToxB. Samples were collected at 0, 6, 12, 24, 48,
177 and 72 h post-infiltration (hpi), and *Tsc2* mRNA abundance was quantified by quantitative real-
178 time (qRT)-PCR relative to *GAPDH* (Supplementary Table 8; Fig. 5; Supplementary Table 9).
179 *Tsc2* transcript levels in both cohorts declined ~5-fold within six hours (6 hpi), possibly
180 reflecting a transient wound response to the mechanics of the infiltration. Mock-treated leaves
181 subsequently regained expression, returning to baseline by 48 hpi (1.22 ± 0.14-fold) and
182 remaining stable through 72 hpi. In contrast, *Tsc2* transcription in Ptr ToxB-treated tissue
183 remained repressed throughout the time-course, never exceeding 40% of the initial level (0.33 ±
184 0.10 at 24 hpi; 0.17 ± 0.02 at 72 hpi). The divergence was highly significant at 48 hpi (P =
185 0.001) and 72 hpi (P = 0.003). Thus, Ptr ToxB does not appear to induce *Tsc2* expression.
186 Instead, it leads to transcriptional suppression that precedes cell death in Ptr ToxB-sensitive
187 plants.

188

Phylogenetic analysis, domain architecture, and subcellular localization of Tsc2

The plant exocyst is an octameric vesicle-tethering complex composed of Sec3, Sec5, Sec6, Sec8, Sec10, Sec15, Exo70, and Exo84 subunits[39]. During land plant evolution, Exo70 expanded into ten clades (A, B, C, D, E, F, G, H, I, and J), while a further, highly divergent clade, Exo70FX, arose after the Poales order diverged from other monocots and subsequently radiated in the grasses[40]. To establish the evolutionary relationship of *Tsc2*, we appended its amino acid sequence to the FX11/FX12/FX15 data sets reported previously[40] and rebuilt a structure-guided, maximum-likelihood phylogeny (Fig. 6). As can be seen from this analysis, Tsc2 grouped decisively with the FX15 branch, indicating it is an Exo70FX15 isoform.

We next examined whether the Tsc2 protein preserves the architectural signatures of canonical Exo70s. AlphaFold2 modelling, followed by superimposition onto yeast (PDB: 2B1E) and *Arabidopsis* (PDB: 4RL5) Exo70 structures, showed that Tsc2 retains the canonical CAT-B, CAT-C, and CAT-D domains but lacks both the N-terminal CorEx helix and the CAT-A domain (Fig. 6). CorEx forms the four-helix zipper that docks Exo70 onto Exo84 and nucleates exocyst assembly. CAT-A, together with CAT-D, contributes to phospholipid binding at the plasma membrane[39,41]. Loss of both elements suggests that Tsc2 is unlikely to participate in a canonical exocyst and has instead acquired a specialized function.

Consistent with this prediction, a Tsc2-GFP fusion expressed in wheat leaf protoplasts localized to the cytoplasm and nucleus but not to the cell periphery or plasma membrane, whereas GFP alone was distributed throughout the cell (Fig. 6). The nucleocytoplasmic pattern supports the notion that Tsc2 has neo-functionalized and acts outside the canonical vesicle-tethering pathway.

To determine if the Tsc2 protein directly interacts with Ptr ToxB, we conducted a yeast two-hybrid (Y2H) assay using Ptr ToxB as bait and full-length Tsc2 as prey in the Y2HGold strain. No growth was obtained on quadruple-dropout medium, indicating that the two proteins do not interact detectably in yeast (Supplementary Figure 3).

Natural variation in *Tsc2* illuminates the genetic basis of tan spot susceptibility

We evaluated 390 *Triticum* accessions for reaction to Ptr ToxB and genotyped them for the presence/absence of a *Tsc2* allele (Supplementary Tables 10-13). The accessions consisted of 112 hexaploid spring wheat and 58 winter wheat lines (*T. aestivum* ssp. *aestivum*), 99 tetraploid durum wheat lines (*T. turgidum* ssp. *durum*), and 121 tetraploid wheat relatives, including wild emmer [*T. turgidum* L. subsp. *dicoccoides* (Körn. ex Asch. & Graebn.) Thell.], cultivated emmer [*Triticum turgidum* L. subsp. *dicoccum* (Schrank) Thell.], and Persian wheat [*Triticum turgidum* L. subsp. *carthlicum* (Nevski) Á. Löve & D. Löve]. Ptr ToxB-sensitivity was common among spring wheat (41/112, 37%) and durum (52/99, 52%) lines, but it was rare among the winter wheat lines (3/58, 5%) and the tetraploid relatives (2/121, 2%). Gene-specific PCR revealed that the entire *Tsc2* coding region was absent in 221 lines (57% of all lines), all of which were Ptr ToxB-insensitive.

Among the 177 lines that retained an allele of *Tsc2*, Sanger sequencing resolved five haplotypes (Table 1, Fig. 7). The canonical Ptr ToxB-sensitivity allele (Haplotype 1) had a 21-nt deletion compared to all other haplotypes, which all conferred Ptr ToxB-insensitivity. These 21 nts encoded amino acids WSLMVEP at positions 370-376. The deletion was present in 98 lines, all of which were sensitive to Ptr ToxB (Table 1, Supplementary Table 14). Haplotypes 1 and 2 differed only by the 21-nt indel, and the latter was specific to wild emmer wheat. Haplotypes 3,

4, and 5 retained the ancestral 21-nt segment and carried one or more single-nucleotide substitutions, and they were specific to durum wheat, cultivated emmer wheat, and common hexaploid wheat, respectively. Therefore, Ptr ToxB-mediated tan spot susceptibility in wheat appears to be conferred by the 21-nt deletion in the CAT-C domain of *Tsc2*, making it a gain-of-function deletion with regards to Ptr ToxB-sensitivity, whereas complete loss of the gene or retention of the 21-nt segment results in resistance.

To examine the structural consequence of the indel, we compared the predicted protein structures of protein isoforms encoded by Haplotypes 1 and 2, which differ only for the seven-amino acid loop (370-376) encoded by the 21-nt indel. Presence of the seven residues nearly doubles the principal surface cavity (surface area 1,755 $Å^2$; volume 3,318 $Å^3$) (847 $Å^2$; 1,710 $Å^3$) and raises the CavityPlus DrugScore (6,626 versus 1,714), without changing predicted binding energy (mean pK_d ≈ 6.95 in both) (Fig. 7; Supplementary Table 15).

Emergence and spread of the *Tsc2* susceptibility allele

Evaluation of the available genome sequences of the A- and D-genome diploid progenitors, AB tetraploids, and ABD hexaploids indicated that *Tsc2* homoeoalleles do not exist on the homoeologous chromosomes 2A or 2D. However, all B-genome relatives (*Ae. speltoides*, *Ae. sharonensis*) and progenitors (*T. turgidum* ssp. *dicoccoides*) with available genome sequences harbored a *Tsc2* allele that retained the 21-nt segment deleted in the Ptr-ToxB-sensitive allele (Haplotype 1) (data not shown). This indicates that the *Tsc2* allele that confers insensitivity to Ptr ToxB is the primitive form, and sensitivity was acquired upon deletion of the 21-nt segment (Haplotype 1). Because the allele that confers sensitivity to Ptr ToxB did not occur in any of the durum wheat progenitors and was more prevalent among durum cultivars

than hexaploid wheat cultivars, we hypothesized that the deletion giving rise to the Ptr ToxB-sensitive allele occurred in a durum wheat cultivar and was inadvertently introduced into hexaploid wheat through conventional cross hybridization (Fig. 8).

To explore this hypothesis, we evaluated the pedigree of the oldest Ptr ToxB-sensitive hexaploid cultivar in our panel, which was Thatcher (Supplementary Table 10), released in 1935. Evaluation of the lines in the pedigree of Thatcher (Marquis/Iumillo//Marquis/Kanred) indicated that all were Ptr ToxB-insensitive except for Iumillo, which is a durum wheat cultivar released circa 1904 (Supplementary Tables 10, 12, 14). This finding suggests that the 21-nt deletion, which resulted in the Ptr ToxB-sensitive allele, likely occurred first in a domesticated durum cultivar and was inadvertently transferred to common wheat cultivars such as Thatcher, where it was subsequently transferred to additional common wheat cultivars through conventional breeding practices.

Tools for the development of tan spot resistant wheat

Elimination of the *Tsc2* Ptr ToxB-sensitivity allele through conventional selective breeding or disruption of function through gene editing would lead to Ptr ToxB-insensitivity and increased tan spot resistance. Here, we pursued both options to provide tools for wheat researchers to develop tan spot-resistant wheat.

To enable efficient elimination of *Tsc2* in breeding pipelines, we developed a two-step genotyping scheme based on the fluorescence-based absent allele-specific amplification (FAASA) strategy described previously[42]. First, we designed a presence/absence marker (*fcp1066*) targeting the absent allele of *Tsc2* (Fig. 9A). Marker *fcp1066* was applied to three major wheat panels totaling 1,483 lines: the Global Durum Panel (GDP; n = 470), a winter wheat

(WW) panel (n = 235), and a spring wheat (SW) panel (n = 778)[43–45]. Consistent with prior reports, 68.2% of GDP lines[30] and all WW lines were insensitive to Ptr ToxB[44], whereas phenotyping of the SW panel performed in this study revealed that 95.6% were insensitive and 3.9% were sensitive (Supplementary Tables 16-18). Across all three panels, *fcp1066* resolved samples into two separate non-overlapping fluorescence clusters, corresponding to lines lacking *Tsc2* (*Tsc2*-) and lines carrying a *Tsc2* allele (*Tsc2*+) of unknown haplotype (Fig. 9A). All lines classified as *Tsc2*- were insensitive to Ptr ToxB, yielding 100% concordance between the absent allele of *Tsc2* and Ptr ToxB-insensitivity among these sets of diverse wheat germplasm.

Because *Tsc2*+ lines can carry insensitive haplotypes (lacking the 21-nt deletion) or the sensitive haplotype (with 21-nt deletion), we developed a second marker assay (*fcp1077*) to discriminate alleles at the 21-nt indel within the CAT-C domain. This assay robustly separated the deletion allele (-21-nt; Ptr ToxB-sensitive Haplotype 1) from the ancestral allele (+21-nt; Ptr ToxB-insensitive Haplotypes 2-5) among *Tsc2*+ lines (Fig. 9B). In the durum panel, for example, lines with the -21-nt allele corresponded to Haplotype 1 and were uniformly sensitive, whereas lines with the +21-nt allele carried Haplotype 3 and were insensitive (Table 1, Supplementary Tables 14, 16).

In parallel, we established a gene-editing approach to eliminate *Tsc2* function. Using CRISPR/Cas9, we introduced a single-base insertion (g.39_40insC) near the 5′ end of the *Tsc2* coding sequence in Kronos, resulting in a frameshift and premature stop codon (Fig. 9C). The predicted truncated protein lacked almost the entire Exo70 core. Plants homozygous for this edited allele showed complete loss of Ptr ToxB-induced chlorosis compared to wild-type Kronos, confirming that CRISPR/Cas9-mediated disruption of *Tsc2* is sufficient to convert a sensitive line into an insensitive one. Together, these marker-assisted and gene-editing tools

provide complementary, breeder-ready strategies to eliminate *Tsc2*-mediated tan spot susceptibility in wheat.

Discussion

The identification of *Tsc2* as a member of the Exo70 subunit family marks a significant expansion of the known classes of disease susceptibility genes in plants. Previously characterized NE-recognizing susceptibility genes had, until now, been confined to proteins that contain PK domains, presumably involved in signaling, and other domains likely involved in protein-protein interactions, such as LRR and major sperm protein (MSP) domains[21,46]. In contrast, *Tsc2* encodes an Exo70 subunit of the exocyst complex, a fundamentally different protein class lacking any obvious receptor or enzyme activity. This finding broadens the paradigm of NE-triggered susceptibility beyond the typical perception-type genes and underscores the ability of necrotrophic pathogens to hijack diverse host proteins to induce susceptibility.

Tsc2 resides in the grass-specific Exo70FX clade, a lineage that emerged after the monocot-dicot split and proliferated in Poales[40,47]. The biological specialization of many Exo70FX members remains unclear, but recent studies suggest roles in plant immunity[40,48]. In barley, an Exo70FX protein (HvExo70FX12) was found to be indispensable for resistance against wheat stripe rust (*Puccinia striiformis*), acting in concert with an LRR-RLK to mediate race-specific immunity[40]. This finding implies that certain Exo70FX isoforms have evolved to partner with immune receptors or pathways, perhaps as adaptively evolved "secretory hubs" in defense. Exo70FX members have also been identified as integrated domains in NLR proteins, suggesting a role in pathogen recognition leading to ETI[49]. By contrast, the function of the Exo70FX15 protein encoded by *Tsc2* is exploited by Ptr to induce susceptibility. Interestingly,

phylogenetic analyses show that the wheat Exo70FX15 and barley Exo70FX12 proteins are closely related sister variants that recently diverged from Exo70FX11 within the FX clade. Their repeated duplication and subsequent neofunctionalization in Triticeae likely stem from selection pressures imposed by pathogens[40,48].

Classical exocyst components typically reside at or near the plasma membrane, using phospholipid-binding domains to tether vesicles[39,41,50]. In many plants, Exo70A1 and Exo70B2 cluster at the cell periphery and mark sites of exocyst assembly[41,51]. By contrast, Tsc2 lacks the CorEx and CAT-A domains which are required to drive the membrane-bound vesicles to the plasma membrane[39]. A parallel observation was made previously[40] for barley HvExo70FX12, which lacks the CorEx and CAT-A domains integral to exocyst assembly, indicating a specialized receptor-kinase immunity pathway rather than typical exocytosis[48]. We found that Tsc2 localizes to the nucleus and cytoplasm but not the plasma membrane, indicating that it may operate in intracellular signaling processes rather than direct pathogen contact. Because Ptr ToxB is known to remain in the apoplast[34], it is possible that an unknown wheat RLK or receptor-like protein could perceive Ptr ToxB at the plasma membrane and subsequently recruit Tsc2 through direct or indirect interaction to trigger downstream defense signaling.

When hexaploid wheat (*T. aestivum*) formed ~10,000 years ago from the hybridization of an AB tetraploid wheat with *Ae. tauschii,* it likely acquired the primitive *Tsc2* allele, which contained the critical 21-nt segment and was insensitive to Ptr ToxB. Because the Ptr ToxB-sensitive allele (Haplotype 1) is much more prevalent in durum cultivars (~32%) than in the durum progenitors (0%) and hexaploid wheat cultivars (<5%), we hypothesize that the critical 21-nt deletion that gave rise to the Ptr ToxB-sensitive allele occurred in a domesticated durum cultivar and was subsequently introgressed into modern hexaploid wheat varieties through

conventional breeding practices. Our finding that the hexaploid spring wheat cultivar Thatcher likely obtained the *Tsc2* susceptibility allele from the Ptr ToxB-sensitive durum variety Iumillo supports this hypothesis. Iumillo was used in the development of Thatcher to transfer stem rust resistance[52], and Ptr ToxB-sensitivity conferred by Haplotype 1 of the *Tsc2* allele was concomitantly transferred. Thatcher became a dominant cultivar in the Great Plains of the USA and Canada for several decades because of its good levels of stem rust resistance, and it was widely used in HRSW breeding programs[53]. Therefore, it is possible that Thatcher served as a hexaploid source for the *Tsc2* susceptibility allele to be incorporated into other HRSW lines. However, this is only one scenario, and it is possible that additional events occurred that moved the susceptible allele from durum to hexaploid wheat lines.

For decades, vulnerability to tan spot remained hidden; partially because of intensive tillage and burning of crop residues that kept residue-borne pathogens in check[12,13], and Ptr races carrying Ptr ToxB were not prevalent. The shift to reduced tillage and continuous cropping in the 1970s changed that calculus, boosting Ptr inoculum and exposing the functionality of *Tsc2* in many Thatcher derivatives[5,25]. Today, Ptr ToxB-sensitivity is still rare in winter wheat but reaches 4-9 % in spring wheat panels[44,54], mirroring the global footprint of Thatcher germplasm. Thus, a seven-codon deletion that likely arose in durum and rode into hexaploid wheat on the coattails of rust resistance now poses a major foliar disease threat.

Most modern wheat breeders employ genomic and marker-assisted selection using high-throughput platforms consisting of thousands of markers. Together, marker assays *fcp1066* and *fcp1077* provide a simple two-step process for breeders to characterize their lines for *Tsc2*. First, they can use the *fcp1066* assay to identify all *Tsc2*- lines as inherently Ptr ToxB-insensitive. If deeper selection is desired, they can then screen the *Tsc2*+ lines with the *fcp1077* assay to

identify lines carrying the deleterious -21-nt susceptibility allele. The ability to identify lines lacking *Tsc2* with 100% accuracy eliminates the need for time-consuming infiltration assays, ensuring that only lines insensitive to Ptr ToxB advance in breeding pipelines. These marker assays can be readily incorporated into established marker-assisted and genomic selection pipelines and therefore provide a promising solution for most wheat breeding programs to minimize tan spot susceptibility. In this capacity, our study provides a cost-effective and straightforward strategy to substantially improve tan spot resistance.

We also demonstrated that gene editing can be used to effectively 'turn off' *Tsc2* to generate a Ptr ToxB-insensitive allele. Should gene editing methods in wheat become socially and politically accepted, this technology may prove efficient for disrupting disease susceptibility genes in wheat cultivars in a targeted and focused manner, as opposed to conventional breeding practices that run the risk of introducing undesirable alleles at other loci, just as the Ptr ToxB-sensitive allele of *Tsc2* was inadvertently introduced into Thatcher wheat. Because *Tsc2* absent alleles are quite common in nature, it is unlikely that the present *Tsc2* alleles of any haplotype have a critical function. However, if it were to be discovered in the future that a particular *Tsc2* allele was beneficial under certain conditions, gene editing may serve as an important tool for the generation of novel alleles that may serve the newly discovered beneficial function as well as insensitivity to Ptr ToxB. Allele engineering could also take into account the ability to develop a high-throughput marker for that allele.

Overall, this work shows that a neofunctionalized plant exocyst component underwent a gain-of-function mutation in the form of a 21-nt deletion that allowed it to be hijacked by a pathogen effector, resulting in the exacerbation of disease. Not only does this work shed light on the role of *Tsc2* in Ptr ToxB-induced tan spot susceptibility, but it also broadens our

understanding of host targets exploited by necrotrophic pathogens. By illustrating how a single exocyst subunit can function as a susceptibility factor, this study also highlights the remarkable evolutionary plasticity of the exocyst complex and suggests that further investigation of other Exo70FX subfamily members will likely deepen our understanding of plant disease resistance and susceptibility mechanisms. From a practical perspective, the knowledge and tools developed in this work will allow wheat breeders to efficiently develop tan spot resistant cultivars in the present and future.

Methods

Plant materials

A durum wheat population of 149 RILs (KG RIL population) derived from Kronos (Ptr ToxB-sensitive) × Gredho (insensitive) was used for initial and saturation mapping of *Tsc2*. The same cross was made to develop an F_2 population for high-resolution mapping. A total of 7,002 F_2 plants were evaluated for reaction to Ptr ToxB, and 1,492 insensitive plants were selected for genotyping. Kronos TILLING lines[38] and the hexaploid wheat cultivar Prosper were used for the evaluation of mutations as described below. For gain-of-function complementation, we used the hexaploid wheat cultivar Fielder as the transformation recipient, and the durum cultivar Kronos was used for gene editing and transcription experiments.

The hexaploid wheat cultivar Jimai 22 was used for subcellular localization experiments. For natural allelic variation analyses and marker validation, we evaluated three germplasm panels totaling 1,483 cultivated lines: a global durum panel (GDP, n = 470), a spring wheat panel (HRSW, n = 778), and a winter wheat panel (WW, n = 235) (Supplementary Tables 16-18). We

418 also examined a diverse set of 121 wild and domesticated tetraploid relatives that included *T.*
419 *turgidum* ssp. *dicoccoides* (n = 6), *dicoccum* (n = 109), and *carthlicum* (n = 6) (Supplementary
420 Table 13).
421
422 **Plant growth and phenotyping**
423 All experiments were conducted in a greenhouse or growth chambers at 21 °C with a 12
424 h photoperiod. Seeds of all lines were sown in Super Cell cone containers (Stuewe & Sons) filled
425 with Sunshine SB100 mix (Sun Gro Horticulture) and supplemented with Osmocote Plus (15-9-
426 12; Scotts). Ptr ToxB cultures were produced and plants were infiltrated and scored as described
427 previously[30].
428
429 **Genomic DNA extraction, genotyping, and linkage mapping in the KG RIL population**
430 DNA was extracted as described previously[55], and genotyping was performed at the
431 USDA-ARS Small Grains Genotyping Lab (Fargo, ND) using the Illumina Infinium iSelect 90K
432 SNP array[56]. GenomeStudio v2.0 was used for clustering and genotype calling. Linkage analysis
433 was carried out in MapDisto v2.1.7 as described previously[57].
434
435 **Saturation mapping and high-resolution mapping**
436 Genomic DNA for all assays was extracted from seedling leaves as described above. SSR
437 markers were mined from the genomic sequence flanking the *Tsc2* region in the *T. turgidum* cv.
438 Kronos and the synthetic hexaploid W7984 assemblies[37,58]. SSRs were identified with Krait
439 v1.3.3, and primers were designed in Krait/Primer3 (https://www.ncbi.nlm.nih.gov/tools/primer-
440 blast/)[59]. Polymorphic SSRs were genotyped across the KG RILs as described previously[23] and

added to the linkage map. KASP assays were developed from SNPs differentiating Kronos and Gredho using publicly available exome-capture data (WheatCAP project 2017_WheatCAP_UCD; https://wheat.triticeaetoolbox.org/) aligned to the Chinese Spring reference (IWGSC RefSeq v1.0; https://graingenes.org/). Assays were designed with PolyMarker[60] to ensure genome specificity. Primer sequences and all SSR/KASP marker positions are listed in Supplementary Table 3.

Kronos × Gredho F_2 plants were infiltrated with Ptr ToxB and classified as sensitive or insensitive. A total of 1,492 plants were insensitive and therefore homozygous recessive at *Tsc2*. Flanking markers *fcp1028* and *fcp1033* were used to screen the 1,492 F_2 plants to identify crossovers, and all recombinants were genotyped with the full interval marker set.

Comparative genomics

We analyzed the candidate gene region in 12 sequenced lines: four Ptr ToxB-sensitive lines (Kronos, Simeto, Glenn, SY Mattis v1.0) and eight Ptr ToxB-insensitive lines (ArinaLrFor v3.0, CDC Landmark v1.0, Chinese Spring v2.1, Fielder, Jagger v1.0, Julius v1.0, LongReach Lancer v1.0, Svevo v1.0) (Supplementary Table 5). Public assemblies were obtained from GrainGenes (https://graingenes.org/), Wheatomics (http://wheatomics.sdau.edu.cn/), and Ensembl Plants (https://plants.ensembl.org/), and scaffold assemblies for Simeto and Glenn were provided by USDA-ARS (Fargo, ND). Where available, existing GFF3 annotations were used. For unannotated assemblies, gene models were predicted with AUGUSTUS (https://bioinf.uni-greifswald.de/augustus/) using wheat parameters. Predicted coding sequences were translated and functionally annotated using the NCBI Conserved Domain Database and InterProScan

v5.52-86.0. Following established criteria[23], features <500 bp or lacking Pfam support at $E < 1\times10^{-5}$ were classified as pseudogenes/fragments and excluded from downstream comparison.

Orthology and presence-absence were assessed by BLAST (nucleotide and protein) against Kronos (genome v1.1) gene models[37], recording percent identity and query coverage. Multiple sequence alignments were used to examine large polymorphisms (insertions/deletions, truncations) within coding regions. Genes conserved across all 12 genomes were recorded as shared; genes present and intact in all sensitive lines but absent or structurally disrupted in insensitive lines were flagged as candidates for *Tsc2* (Supplementary Table 5).

EMS and TILLING mutant screening

Kronos TILLING lines[38] were queried for nonsense or predicted deleterious missense variants in *TrturKRN2B01G009130* (LRR-RLK) (n = 19 lines) and *TrturKRN2B01G009140* (*TtExo70FX15*) (n = 10 lines) (Supplementary Tables 6 and 7). Mutant families were grown and assayed for Ptr ToxB reaction. Candidate lines were verified by Sanger sequencing of the target amplicon. The insensitive families were re-tested in the next generation to confirm the phenotype. A Prosper EMS population of 1,050 M_2 families, previously developed[22], was evaluated for sensitivity to Ptr ToxB. Fourteen seeds from each family were infiltrated with Ptr ToxB, and *TaExo70FX15* was sequenced from insensitive plants using Sanger sequencing and aligned with wild-type Prosper sequences. Variants in Kronos TILLING and Prosper EMS lines were classified as synonymous, missense, or nonsense. Missense variants were evaluated with SIFT[61] and inspected with Missense-3D (https://missense3d.bc.ic.ac.uk/) and DynaMut2 (https://biosig.lab.uq.edu.au/dynamut2/) for predicted structural impacts as described previously[62].

Agrobacterium-mediated transformation and functional complementation of *Tsc2*

A 6,468-bp genomic fragment comprising the complete *Tsc2* open reading frame plus 2,734 bp upstream and 2,231 bp downstream sequences was PCR-amplified from Kronos genomic DNA with Phusion® High-Fidelity polymerase (New England Biolabs). Primers were designed with overhangs compatible with the In-Fusion® HD Cloning system (Takara Bio USA, Inc.). The binary vector pCAMBIA1300-ubi-GRF-GIF[63] was linearized with *Kpn*I and *Spe*I (New England Biolabs) and purified using the Wizard® SV Gel and PCR Clean-Up System. The purified insert was then ligated into the linearized vector using the In-Fusion® Snap Assembly (Takara Bio USA, Inc.) according to the manufacturer's protocols. The recombinant plasmid was introduced into NEB 5-alpha Competent *E. coli* cells (New England Biolabs) via heat shock transformation, and colony PCR was used to verify successful transformants. Plasmid DNA from confirmed clones was extracted using the QIAprep Spin Miniprep Kit (Qiagen). The complete construct was then validated by whole-plasmid sequencing (Eurofins Genomics) to ensure the correct insertion of the 6,468 bp fragment. The validated recombinant plasmid was subsequently introduced into *Agrobacterium tumefaciens* strain AGL1T[64] by electroporation.

Single colonies were verified by PCR, propagated in LB (kanamycin + rifampicin), and stored in 15 % glycerol at -80 °C. Transformation was performed using a previously described protocol[65], with minor adjustments. Briefly, immature Fielder embryos (~14 d post-anthesis) were excised after surface sterilization and inoculated with AGL1T containing the construct (OD_{600} ~ 0.5, 100 µM acetosyringone, 0.05 % Silwet L-77). After 3 days of co-cultivation at 24 °C in the dark, embryos were rested for 5 days on wheat callus-induction medium (WCI). Hygromycin selection was then carried out on WCI containing 15 mg/L hygromycin for 2 weeks

in the dark, followed by selection on WCI supplemented with 30 mg/L hygromycin for an additional 3 weeks, consisting of 2 weeks in the dark and 1 week under weak light conditions. Hygromycin-resistant calli with green foci were transferred to wheat regeneration medium (WRM + 0.5 mg/L Zeatin); recalcitrant calli were transferred to WRM supplemented with 1 mg/L zeatin. Shoots with roots were hardened on hygromycin (15 mg/L) rooting medium, then transplanted to vermiculite and finally to soil (22 °C, 16 h light). T_0 plants were screened at the two- to three-leaf stage by leaf infiltration with Ptr ToxB infiltration of individual leaves from each tiller (described above). Following phenotypic scoring, leaf tissue from each infiltrated tiller was collected, and the presence of the transgene was verified by PCR with *Tsc2*-specific primers (Supplementary Table 19) and Sanger sequencing.

RNA isolation, first-strand cDNA synthesis, and RACE cloning

To investigate the expression pattern of *Tsc2* across wheat tissues, samples were collected from the durum wheat cultivar Kronos. Leaf and root tissues were harvested from two-week-old seedlings, stem tissue was collected at Feekes growth stage 7 (two nodes detectable; https://nutrien-ekonomics.com/infographics/wheat-growth/), and immature spike tissue was collected at Feekes growth stage 9 (flag leaf ligule just visible).

Total RNA was extracted and cDNA prepared from Kronos tissues as described in Zhang et al.[46]. RT-PCR amplification was performed using gene-specific primers for *Tsc2* and the housekeeping gene *GAPDH*, which served as an endogenous control (primer sequences listed in Supplementary Table 19). The *GAPDH* primers were designed to distinguish cDNA from genomic DNA, yielding a 187-bp product from cDNA and a 357-bp product from genomic DNA[17]. PCR products were resolved by agarose gel electrophoresis to verify amplification

specificity. Detection of the expected cDNA-sized *GAPDH* amplicon confirmed successful reverse transcription.

For RACE cloning, *Tsc2* coding sequences were amplified with gene-specific primers (Supplementary Table 19), purified from 1.5 % agarose gels, and recovered with the Wizard® SV Gel & PCR Clean-Up kit (Promega). 5′- and 3′-UTRs were evaluated using the SMART RACE (SMARTer RACE 5′/3′ Kit; Takara Bio USA). Reads were assembled in Geneious Prime 2025.1.3 (https://www.geneious.com) to obtain the full-length *Tsc2* cDNA, delineate the 5′/3′ UTRs, and define exon-intron boundaries by alignment to the genomic sequence.

qRT-PCR assay

cDNA from Kronos leaf was serially diluted (1:2, 1:4, 1:8, 1:16, 1:32). Reactions (10 µL) contained 5 µL SYBR™ Select Master Mix (Thermo Fisher Scientific), 0.5 µM each primer (for *Tsc2* or *GAPDH*), and 2 µL diluted cDNA, and were run on a Bio-Rad CFX384™ system with: 95 °C 2 min; 40 cycles of 95 °C 15 s, 60 °C 1 min; followed by a melt curve (65-95 °C, 0.5 °C increments). Standard-curve slopes yielded amplification efficiencies within 90-110% for both targets, permitting ΔΔCq-based relative quantification in the time course.

For the temporal experiment, secondary leaves of two-week-old Kronos plants were infiltrated with Ptr ToxB or YPD media (mock). Tissue was collected at 0, 6, 12, 24, 48, and 72 hpi. For each time point and treatment, 5-7 biological replicates were analyzed, with ≥3 technical replicates per sample. Cq values were averaged across technical replicates and normalized to *GAPDH* (ΔCq). Cq values were exported from Bio-Rad CFX Maestro 2.3 (Version: 5.3.022.1030) and analyzed by the ΔΔCq method. *Tsc2* was normalized to *GAPDH*, which showed stable expression across samples. The 0 hpi YPD group was used as the calibrator, and

fold change was calculated as $2^{-\Delta\Delta Cq}$. Group means and SEM were visualized from biological replicates (5-7 per treatment and time point). Between-treatment differences at each time point were evaluated with two-sided Welch's *t*-tests in '*scipy.stats*'.

3D-structure of Tsc2 and phylogenetic analysis

The Tsc2 protein was modelled with AlphaFold2 via ColabFold v1.5.2-patch pipeline[66,67] using default settings, and the highest-confidence model (pLDDT and PAE) was used for analysis as described previously[62]. Protein structures were generated to predict the wild-type TtExo70FX15 (Tsc2) protein, and missense mutations were mapped onto the predicted structure to visualize their spatial positions (Supplementary Figures 1 and 2). To place Tsc2 within the Exo70 structural framework, the predicted model was aligned to yeast Exo70 (PDB 2B1E) and *Arabidopsis* EXO70A1 (PDB 4RL5) using TM-align (https://www.rcsb.org/alignment), and superpositions were examined in UCSF ChimeraX v1.6.1 (https://www.cgl.ucsf.edu/chimerax/). Exo70 subdomains (CorEx, CAT-A to CAT-D) were assigned by transferring domain boundaries from yeast Exo70 onto the aligned Tsc2 structure and refining these boundaries using MAFFT-DASH structure-guided alignments and ChimeraX Matchmaker, following the approach described in Bergum et al.[48].

To evaluate the structural consequences of natural variation, additional AlphaFold2 models were generated for the +21-nt (ancestral) and -21-nt (deletion) alleles. Missense mutations identified in TILLING and EMS populations were mapped onto the wild-type TtExo70FX15 structure to visualize their spatial positions. Missense effects were assessed with SIFT[61], Missense3D (https://missense3d.bc.ic.ac.uk/), and DynaMut2 (https://biosig.lab.uq.edu.au/dynamut2/) as described by Seneviratne et al.[62]. The impact of the

21-nt indel on protein architecture was further examined using cavity predictions from CavityPlus with default parameters as described previously[46], and for each allele, the highest-scoring cavity was recorded (volume, surface area, DrugScore). All structural visualizations were prepared in UCSF ChimeraX v1.6.1.

For phylogenetic analysis, Tsc2 was incorporated into the Exo70FX11/FX12/FX15 data sets from Holden et al.[40]. Sequences were aligned with MAFFT-DASH v7.520 using structure-based alignment as described by Bergum et al.[48], filtered to remove redundant sequences, and trimmed to exclude poorly aligned positions. Maximum-likelihood trees were inferred using RAxML v8.2.12 with the GAMMA model of rate heterogeneity and 1,000 bootstrap replicates. Phylogenies were visualized and annotated using iTOL v7.3 (https://itol.embl.de/).

Subcellular localization of Tsc2 protein

Transient expression of an N-terminal GFP fusion of Tsc2 (35S::pAN580-Tsc2-GFP) was outsourced to Lifeasible (Shirley, NY, USA; www.lifeasible.com) and carried out as described by Zhang et al.[46]. In brief, mesophyll protoplasts were isolated from 10- to 15-day-old seedlings of wheat cv. Jimai 22, transformed with the fusion construct by PEG-mediated uptake, incubated for 18-24 h at 24 °C, and examined with fluorescence or laser-scanning confocal microscopy to visualize GFP signal and determine the subcellular localization of Tsc2.

Yeast two-hybrid

Assessment of the physical interaction between Tsc2 (TtExo70FX15) and Ptr ToxB was subcontracted to Lifeasible (Shirley, NY, USA; www.lifeasible.com) and followed the Matchmaker Gold Yeast Two-Hybrid System protocol detailed by Zhang et al.[46]. In brief, ToxB

cDNA was fused to the GAL4 DNA-binding domain in pGBKT7 (bait), while Tsc2 cDNA was fused to the GAL4 activation domain in pGADT7 (prey). Auto-activation and toxicity of the bait construct were evaluated prior to interaction testing. Bait and prey plasmids were co-transformed into the Y2HGold yeast strain, and transformants were selected on SD/-Leu/-Trp medium. Protein-protein interactions were assessed using the HIS3, ADE2, and lacZ reporter genes.

Allelic variation and haplotype analysis

The *Tsc2* coding region was PCR-amplified from 391 *Triticum* accessions (Supplementary Tables 10-13) using gene-specific primers spanning the full ORF (Supplementary Table 19) to determine the presence/absence of *Tsc2* alleles. Amplicons were sequenced from the 177 accessions that harbored a *Tsc2* allele. Reads were assembled in Geneious Prime to produce high-quality consensus sequences, translated, and aligned with MAFFT. Haplotypes were defined by the presence/absence of the 21-nt indel in CAT-C and by nonsynonymous SNPs (Supplementary Table 14).

Development and evaluation of diagnostic FAASA marker assays

Two KASP-based FAASA multiplex assays were developed to enable high-throughput genotyping of *Tsc2*: *fcp1066*, which detects the presence/absence of the *Tsc2* gene, and *fcp1077*, which targets the diagnostic 21-nt indel within the gene. Both assays were designed using the FAASA framework[42], in which a four-primer system is used to simultaneously amplify the target region and a conserved internal control. Each assay consisted of a pair of *Tsc2* target-specific primers (TSPs) and a pair of primers targeting the wheat *Q* gene (core gene-specific primers, CGSPs). The TSP forward primer carried a 5′ FAM tail, and the CGSP forward primer carried a

5′ HEX tail, enabling fluorescence-based discrimination of *Tsc2* and the internal control. Primer sequences for both markers are listed in Supplementary Table 19. Reactions were assembled and run according to the FAASA cycling conditions described by Running et al.[42].

For *fcp1066*, samples producing only the HEX signal were scored as *Tsc2*-absent, whereas samples producing both HEX and FAM signals were scored as *Tsc2*-present. This marker was validated across all three germplasm panels described above (GDP, WW, SW; n = 1,483). Marker *fcp1077* was designed to discriminate the 21-nt deletion (Ptr ToxB-sensitive) from the ancestral 21-nt insertion (Ptr ToxB-insensitive) within *Tsc2*, using the same FAASA multiplex design. Validation was performed using the durum panel, where allele calls matched the Ptr ToxB phenotypes with complete concordance. Because the indel is conserved across wheat subgenomes and the assay relies on the same core FAASA architecture as *fcp1066*, *fcp1077* is expected to perform robustly in additional germplasm.

Gene editing using CRISPR/Cas9

CRISPR/Cas9 editing of *Tsc2* was carried out using the pCBC-MT1T2 gRNA assembly system[68] and the JD633 CRISPR/Cas9 vector containing the GRF-GIF cassette[63]. Gene-specific target sequences were incorporated into the MT1 and MT2 gRNA modules by PCR, and the resulting 966-bp product was gel-purified and assembled into JD633 using Golden Gate cloning[69]. All cloned constructs were verified by whole-plasmid nanopore sequencing (https://eurofinsgenomics.com) prior to *Agrobacterium* transformation. The validated CRISPR/Cas9 plasmid was introduced into *A. tumefaciens* strain AGL1T by electroporation, and single colonies were verified by PCR. Wheat transformation was performed in Kronos following the same *Agrobacterium*-mediated protocol described above for functional complementation,

using identical embryo preparation, co-cultivation, selection, regeneration, and acclimation conditions.

Putative T_0 plants were genotyped by PCR using primers flanking the CRISPR target region, and amplicons were sequenced to identify editing events. Phenotyping of T_0 leaves by infiltration with Ptr ToxB (as described above) was performed in parallel to assess sensitivity. A single-base insertion at genomic position g.39_40 was recovered, producing a frameshift and premature stop codon in *Tsc2*. The T_0 plant was self-pollinated, and the T_1 progenies were screened using the same flanking primers. T_1 plants were phenotyped with Ptr ToxB, and sequencing confirmed that homozygous mutants exhibited complete insensitivity, whereas plants carrying the wild-type allele remained sensitive to Ptr ToxB.

Data availability

All data supporting the findings of this study are available within the article and its Supplementary information files. The *Tsc2* haplotype sequences generated from 177 accessions have been deposited in GenBank (https://www.ncbi.nlm.nih.gov/genbank/) under accession numbers PV543977-PV544011, PV544013-PV544024, PV544026-PV544057, PV544059-PV544080, PV544082-PV544091, PV544093-PV544116, PV544118-PV544138, and PV544140-PV544160. All genetic materials generated and used in this study are available from the corresponding author upon reasonable request and completion of a material transfer agreement (MTA).

Code availability

No custom code was generated in this study.

Author contributions

G.S. and J.D.F. conceived and designed the study. G.S., K.L.D.R., S.S., K.A., T.M.R., A.R.P.H., Z.Z., A.S.-H., and P.K. conducted the experiments and collected the data. Z.L., P.E.M., and S.Y. contributed resources. G.S. analyzed and interpreted the data with input from K.L.D.R., S.S., Z.L., S.Y., and J.D.F. G.S. and J.D.F wrote the first draft of the manuscript, and all authors contributed to revisions of the manuscript. All authors read and approved the final version of the manuscript.

Competing interests

The authors declare no competing interests.

Acknowledgements

We thank Jorge Dubcovsky (Department of Plant Sciences, University of California, Davis) for providing the Kronos × Gredho recombinant inbred line population. We thank Ksenia Krasileva (Department of Plant & Microbial Biology, University of California, Berkeley) for providing the Kronos genome sequence data. We are grateful to Matthew J. Moscou (USDA-ARS Cereal Disease Laboratory & University of Minnesota) and Molly Bergum (The Sainsbury Laboratory, University of East Anglia) for their helpful discussions. We also thank Tessa Burch-Smith (Donald Danforth Plant Science Center) for insightful comments and advice on protein subcellular localization. We would like to thank Gongjun Shi, Stephanie McCoy, Heaven James, and Ava Wiitamaki for technical assistance. This research work was supported by USDA-Agricultural Research Service Current Research Information System (CRIS) project 3060-

693 21000-046-000D. Mention of trade names or commercial products in this publication is solely
694 for the purpose of providing specific information and does not imply recommendation or
695 endorsement by the U.S. Department of Agriculture. USDA is an equal opportunity provider and
696 employer.
697

References

1. Erenstein, O., Chamberlin, J. & Sonder, K. Estimating the global number and distribution of maize and wheat farms. *Glob. Food Secur.* **30**, 100558 (2021).

2. Minter, F. & Saunders, D. G. Safeguarding wheat yields from cereal fungal invaders in the postgenomic era. *Curr. Opin. Microbiol.* **73**, 102310 (2023).

3. De Wolf, E. D., Effertz, R. J., Ali, S. & Francl, L. J. Vistas of tan spot research. *Can. J. Plant Pathol.* **20**, 349–370 (1998).

4. Strelkov, S. E. & Lamari, L. Host–parasite interactions in tan spot [*Pyrenophora tritici-repentis*] of wheat. *Can. J. Plant Pathol.* **25**, 339–349 (2003).

5. Faris, J. D., Liu, Z. & Xu, S. S. Genetics of tan spot resistance in wheat. *Theor. Appl. Genet.* **126**, 2197–2217 (2013).

6. Savary, S. *et al.* The global burden of pathogens and pests on major food crops. *Nat. Ecol. Evol.* **3**, 430–439 (2019).

7. Wulff, B. B. & Krattinger, S. G. The long road to engineering durable disease resistance in wheat. *Curr. Opin. Biotechnol.* **73**, 270–275 (2022).

8. Hosford, R. M. Jr. Tan spot-developing knowledge 1902–1981, virulent races and differentials, methodology, rating systems, other leaf diseases, literature. in *Tan spot of wheat and related diseases workshop* 1–24 (North Dakota Agricultural Experiment Station, Fargo, ND, 1982).

9. Evans, C. K., Hunger, R. M. & Siegerist, W. C. Comparison of greenhouse and field testing to identify wheat resistant to tan spot. *Plant Dis.* **83**, 269–273 (1999).

10. Wegulo, S. N., Breathnach, J. A. & Baenziger, P. S. Effect of growth stage on the relationship between tan spot and spot blotch severity and yield in winter wheat. *Crop Prot.* **28**, 696–702 (2009).

11. Ciuffetti, L. M. *et al. Pyrenophora tritici-repentis*: A plant pathogenic fungus with global impact. in *Genomics of Plant-Associated Fungi: Monocot Pathogens* (eds Dean, R. A., Lichens-Park, A. & Kole, C.) 1–39 (Springer Berlin Heidelberg, Berlin, Heidelberg, 2014). doi:10.1007/978-3-662-44053-7_1.

12. Rees, R., Platz, G. & Mayer, R. Yield losses in wheat from yellow spot: comparison of estimates derived from single tillers and plots. *Aust. J. Agric. Res.* **33**, 899–908 (1982).

13. Sutton, J. C. & Vyn, T. J. Crop sequences and tillage practices in relation to diseases of winter wheat in Ontario. *Can. J. Plant Pathol.* **12**, 358–368 (1990).

14. Jørgensen, L. N. & Olsen, L. V. Control of tan spot (*Drechslera tritici-repentis*) using cultivar resistance, tillage methods and fungicides. *Crop Prot.* **26**, 1606–1616 (2007).

15. Lamey, H. A. & McMullen, M. P. *Crop Rotations for Managing Plant Disease*. http://hdl.handle.net/10365/17693 (2011).

16. Singh, P. K., Duveiller, E. & Singh, R. P. Resistance breeding for tan spot (*Pyrenophora tritici-repentis*) of wheat. in *Disease resistance in wheat* (ed. Sharma, I.) 136–150 (CABI, UK, 2012). doi:10.1079/9781845938185.0136.

17. Faris, J. D. *et al.* A unique wheat disease resistance-like gene governs effector-triggered susceptibility to necrotrophic pathogens. *Proc. Natl. Acad. Sci.* **107**, 13544–13549 (2010).

18. Ciuffetti, L. M., Manning, V. A., Pandelova, I., Betts, M. F. & Martinez, J. P. Host-selective toxins, Ptr ToxA and Ptr ToxB, as necrotrophic effectors in the *Pyrenophora tritici-repentis*– wheat interaction. *New Phytol.* **187**, 911–919 (2010).

19. Strelkov, S. E., Lamari, L., Sayoud, R. & Smith, R. B. Comparative virulence of chlorosis-inducing races of *Pyrenophora tritici-repentis*. *Can. J. Plant Pathol.* **24**, 29–35 (2002).

20. Shi, G. *et al.* A Conserved Hypothetical Gene Is Required but Not Sufficient for Ptr ToxC Production in *Pyrenophora tritici-repentis*. *Mol. Plant-Microbe Interactions®* **35**, 336–348 (2022).

21. Faris, J. D. & Friesen, T. L. Plant genes hijacked by necrotrophic fungal pathogens. *Curr. Opin. Plant Biol.* **56**, 74–80 (2020).

22. Running, K. L. D. Genomic characterization of necrotrophic effector sensitivity genes in wheat. (North Dakota State University, Fargo, ND, USA, 2022).

23. Running, K. L. D. *et al.* Genomic analysis and delineation of the tan spot susceptibility locus *Tsc1* in wheat. *Front. Plant Sci.* **13**, 793925 (2022).

24. Friesen, T. L. & Faris, J. D. Molecular mapping of resistance to *Pyrenophora tritici-repentis* race 5 and sensitivity to Ptr ToxB in wheat. *Theor. Appl. Genet.* **109**, 464–471 (2004).

25. Lamari, L., McCallum, B. D. & dePauw, R. M. Forensic pathology of Canadian bread wheat: the case of tan spot. *Phytopathology®* **95**, 144–152 (2005).

26. Abeysekara, N. S., Friesen, T. L., Liu, Z., McClean, P. E. & Faris, J. D. Marker development and saturation mapping of the tan spot Ptr ToxB sensitivity locus *Tsc2* in hexaploid wheat. *Plant Genome* **3**, plantgenome2010.07.0017 (2010).

27. Corsi, B. *et al.* Genetic analysis of wheat sensitivity to the ToxB fungal effector from Pyrenophora tritici-repentis, the causal agent of tan spot. *Theor. Appl. Genet.* **133**, 935–950 (2020).

28. Virdi, S. K. *et al.* New insights into the roles of host gene-necrotrophic effector interactions in governing susceptibility of durum wheat to tan spot and septoria nodorum blotch. *G3 GenesGenomesGenetics* **6**, 4139–4150 (2016).

29. Galagedara, N. *et al.* Genome-wide association mapping of tan spot resistance in a worldwide collection of durum wheat. *Theor. Appl. Genet.* **133**, 2227–2237 (2020).

30. Szabo-Hever, A. *et al.* Association mapping of resistance to tan spot in the global durum panel. *Phytopathology*® PHYTO-02-23-0043-R (2023) doi:10.1094/PHYTO-02-23-0043-R.

31. Gourlie, R. *et al.* The pangenome of the wheat pathogen *Pyrenophora tritici-repentis* reveals novel transposons associated with necrotrophic effectors ToxA and ToxB. *BMC Biol.* **20**, 239 (2022).

32. Strelkov, S. E., Kowatsch, R. F., Ballance, G. M. & Lamari, L. Characterization of the ToxB gene from North African and Canadian isolates of *Pyrenophora tritici-repentis*. *Physiol. Mol. Plant Pathol.* **67**, 164–170 (2005).

33. Hafez, M. *et al.* Evolution of the *ToxB* gene in *Pyrenophora tritici-repentis* and related species. *Mol. Plant-Microbe Interactions*® **37**, 327–337 (2024).

34. Figueroa, M., Manning, V. A., Pandelova, I. & Ciuffetti, L. M. Persistence of the host-selective toxin Ptr ToxB in the apoplast. *Mol. Plant-Microbe Interactions*® **28**, 1082–1090 (2015).

35. See, P. T., Iagallo, E. M., Oliver, R. P. & Moffat, C. S. Heterologous expression of the *Pyrenophora tritici-repentis* effector proteins ToxA and ToxB, and the prevalence of effector sensitivity in Australian cereal crops. *Front. Microbiol.* **10**, 182 (2019).

36. Martinez, J. P., Ottum, S. A., Ali, S., Francl, L. J. & Ciuffetti, L. M. Characterization of the *ToxB* gene from *Pyrenophora tritici-repentis*. *Mol. Plant-Microbe Interactions*® **14**, 675–677 (2001).

37. Seong, K., Kumar, R., Lunde, C. & Krasileva, K. Chromosome-level genome assembly of Triticum turgidum var 'Kronos'. Zenodo https://doi.org/10.5281/ZENODO.11106422 (2024).

38. Krasileva, K. V. *et al.* Uncovering hidden variation in polyploid wheat. *Proc. Natl. Acad. Sci.* **114**, (2017).

39. Mei, K. *et al.* Cryo-EM structure of the exocyst complex. *Nat. Struct. Mol. Biol.* **25**, 139–146 (2018).

40. Holden, S. *et al.* A lineage-specific Exo70 is required for receptor kinase–mediated immunity in barley. *Sci. Adv.* **8**, eabn7258 (2022).

41. Synek, L. *et al.* Plasma membrane phospholipid signature recruits the plant exocyst complex via the EXO70A1 subunit. *Proc. Natl. Acad. Sci.* **118**, e2105287118 (2021).

42. Running, K. L. D. *et al.* Fluorescence-based absent allele-specific amplification (FAASA) for high-throughput detection of absent alleles. *Bio-Protoc.* (2026).

43. Mazzucotelli, E. *et al.* The global durum wheat panel (GDP): an international platform to identify and exchange beneficial alleles. *Front. Plant Sci.* **11**, 569905 (2020).

44. Peters Haugrud, A. R. *et al.* Genome-wide association mapping of resistance to the foliar diseases septoria nodorum blotch and tan spot in a global winter wheat collection. *Mol. Breed.* **43**, 54 (2023).

45. Szabo-Hever, A. *et al.* Evaluation of durum and hard red spring wheat panels for sensitivity to necrotrophic effectors produced by *Parastagonospora nodorum*. *Plant Dis.* **109**, 851–861 (2025).

46. Zhang, Z. *et al.* Protein kinase-major sperm protein (PK-MSP) genes mediate recognition of the fungal necrotrophic effector SnTox3 to cause septoria nodorum blotch in wheat. *Mol. Plant-Microbe Interactions®* **38**, 315–327 (2025).

47. Žárský, V., Sekereš, J., Kubátová, Z., Pečenková, T. & Cvrčková, F. Three subfamilies of exocyst EXO70 family subunits in land plants: early divergence and ongoing functional specialization. *J. Exp. Bot.* erz423 (2019) doi:10.1093/jxb/erz423.

48. Bergum, M. *et al.* Putative neofunctionalization of a Poales-specific EXO70 clade. Preprint at https://doi.org/10.1101/2024.12.13.628418 (2024).

49. Bailey, P. C. *et al.* Dominant integration locus drives continuous diversification of plant immune receptors with exogenous domain fusions. *Genome Biol.* **19**, 23 (2018).

50. Synek, L. *et al.* AtEXO70A1, a member of a family of putative exocyst subunits specifically expanded in land plants, is important for polar growth and plant development. *Plant J.* **48**, 54–72 (2006).

51. Zhang, C. *et al.* Endosidin2 targets conserved exocyst complex subunit EXO70 to inhibit exocytosis. *Proc. Natl. Acad. Sci.* **113**, (2016).

52. Hayes, H. K. *et al. Thatcher Wheat*. 325 (1936).

53. Rouse, M. N., Talbert, L. E., Singh, D. & Sherman, J. D. Complementary epistasis involving *Sr12* explains adult plant resistance to stem rust in Thatcher wheat (*Triticum aestivum* L.). *Theor. Appl. Genet.* **127**, 1549–1559 (2014).

54. Kokhmetova, A. *et al.* Genome-wide association study of tan spot resistance in a hexaploid wheat collection from Kazakhstan. *Front. Genet.* **11**, 581214 (2021).

55. Running, K. L. D. *et al.* Development of diagnostic markers for the disease susceptibility gene Tsn1 in wheat reveals novel resistance alleles and a new locus required for ToxA sensitivity. *Theor. Appl. Genet.* **138**, 164 (2025).

56. Wang, S. *et al.* Characterization of polyploid wheat genomic diversity using a high-density 90,000 single nucleotide polymorphism array. *Plant Biotechnol. J.* **12**, 787–796 (2014).

57. Acharya, K. *et al.* Genetic mapping of QTLs for resistance to bacterial leaf streak in hexaploid wheat. *Theor. Appl. Genet.* **137**, 265 (2024).

58. Chapman, J. A. *et al.* A whole-genome shotgun approach for assembling and anchoring the hexaploid bread wheat genome. *Genome Biol.* **16**, 26 (2015).

59. Du, L., Zhang, C., Liu, Q., Zhang, X. & Yue, B. Krait: an ultrafast tool for genome-wide survey of microsatellites and primer design. *Bioinformatics* **34**, 681–683 (2018).

60. Ramirez-Gonzalez, R. H., Uauy, C. & Caccamo, M. PolyMarker: A fast polyploid primer design pipeline. *Bioinformatics* **31**, 2038–2039 (2015).

61. Ng, P. C. & Henikoff, S. SIFT: predicting amino acid changes that affect protein function. *Nucleic Acids Res.* **31**, 3812–3814 (2003).

62. Seneviratne, S. *et al.* Evolution, diversity, and function of the disease susceptibility gene *Snn1* in wheat. *Plant J.* **119**, 1720–1736 (2024).

63. Debernardi, J. M. *et al.* A GRF–GIF chimeric protein improves the regeneration efficiency of transgenic plants. *Nat. Biotechnol.* **38**, 1274–1279 (2020).

64. Aliu, E., Lee, K. & Wang, K. CRISPR RNA-guided integrase enables high-efficiency targeted genome engineering in *Agrobacterium tumefaciens*. *Plant Biotechnol. J.* **20**, 1916–1927 (2022).

65. Hayta, S. *et al.* An efficient and reproducible *Agrobacterium*-mediated transformation method for hexaploid wheat (*Triticum aestivum* L.). *Plant Methods* **15**, 121 (2019).

66. Mirdita, M. *et al.* ColabFold: making protein folding accessible to all. *Nat. Methods* **19**, 679–682 (2022).

67. Jumper, J. *et al.* Highly accurate protein structure prediction with AlphaFold. *Nature* **596**, 583–589 (2021).

68. Xing, H.-L. *et al.* A CRISPR/Cas9 toolkit for multiplex genome editing in plants. *BMC Plant Biol.* **14**, 327 (2014).

69. Engler, C., Kandzia, R. & Marillonnet, S. A one pot, one step, precision cloning method with high throughput capability. *PLoS ONE* **3**, e3647 (2008).

866

867

868 **Tables**

869

870 **Table 1.** *Tsc2* haplotype distribution across 177 *Triticum* accessions representing five
871 subspecies.
872

Tsc2 haplotype	Length (bp)	Ptr ToxB reaction[b]	N[c]	Wheat class[a]				
				Common wheat	Durum wheat	Cultivated emmer	Wild emmer	Persian wheat
Haplotype 1	1,503	S	98	44	52	0	0	2
Haplotype 2	1,524	I	2	0	0	0	2	0
Haplotype 3	1,524	I	11	0	11	0	0	0
Haplotype 4	1,524	I	22	0	0	22	0	0
Haplotype 5	1,524	I	44	44	0	0	0	0

873

874 [a] Common wheat: *Triticum aestivum*; Durum wheat: *Triticum turgidum* ssp. *durum*; Cultivated
875 emmer: *Triticum turgidum* ssp. *dicoccum*; Wild emmer: *Triticum turgidum* ssp. *dicoccoides*;
876 Persian wheat: *Triticum turgidum* ssp. *carthlicum*. Common wheat is hexaploid and includes
877 both spring and winter types, and all others are tetraploid.
878 [b] Reaction to Ptr ToxB where S = sensitive; I = insensitive.
879 [c] N = Total number of accessions identified with each haplotype.
880

Figure legends

Fig. 1: Phenotypic effects of a compatible *Tsc2*-Ptr ToxB interaction in tetraploid (durum) and hexaploid (common) wheat.
A: Spray inoculation with the Ptr ToxB-producing *Pyrenophora tritici-repentis* race 5 isolate DW5. Wild-type durum wheat cultivar Kronos (tetraploid) and common wheat cultivar Prosper (hexaploid), which carry a functional *Tsc2* allele, exhibit expanding and coalescing chlorotic lesions in response to infection, whereas their corresponding *Tsc2*-disrupted mutants (Kronos2704 and Prosper89a) show infection site lesions with little to no chlorosis development or expansion. **B:** Leaf infiltration of cultures containing the necrotrophic effector Ptr ToxB. Wild-type Kronos and Prosper develop localized cell death at infiltration sites, whereas the *Tsc2*-disrupted mutants undergo no cell death. WT = wild type; Mut = *Tsc2*-disrupted mutant.

Fig. 2: Mapping and identification of candidate genes for *Tsc2*.
A: The initial genetic linkage map of the *Tsc2* region of chromosome arm 2BS generated in the Kronos × Gredho recombinant inbred population. The flanking markers used to define the target interval for marker development are highlighted in yellow. **B:** Saturated linkage map developed in the Kronos × Gredho recombinant inbred population by developing 43 additional markers. **C:** High-resolution linkage map developed in the Kronos × Gredho F_2 population between markers *fcp1023* and *fcp1062*. Along the genetic maps of A, B, and C, marker names are shown above the grey bars, and genetic distances in centimorgan (cM) are shown below. **D:** Physical map of the 108.4 kb candidate interval between markers *fcp1028* and *fcp1033* in the Kronos genome. Blue arrows represent conserved gene models shared between Ptr ToxB-sensitive and -insensitive lines, the green arrow indicates the leucine-rich repeat receptor-like kinase (LRR-RLK; *TrturKRN2B01G009130*), and the dark grey arrow represents the Exo70 family gene subsequently identified as *Tsc2* (*TtExo70FX15*; *TrturKRN2B01G009140*). **E:** The structure of candidate gene *TrturKRN2B01G009140* (*TtExo70FX15*), which consists of a single exon (dark grey). The untranslated regions are indicated by light grey shaded boxes.

Fig. 3: Evaluation and analysis of mutations in the *TtExo70FX15* (*Tsc2*) gene in Kronos and Prosper.
A: Ptr ToxB infiltration reactions and predicted TtExo70FX15 (Tsc2) protein structures of the wild-type wheat lines Kronos and Prosper, and one representative missense mutant in each of the two lines that result in an insensitive reaction to Ptr ToxB. Protein structures depict the AlphaFold-predicted wild-type TtExo70FX15 (Tsc2) protein, with missense mutation sites highlighted to indicate their spatial positions within the structure. The locations of the point mutations in the two mutant proteins are indicated in red and indicated by orange arrows. Infiltration reactions and predicted protein structures for all other Kronos and Prosper *TtExo70FX15* (*Tsc2*) missense mutants are presented in Supplementary Figures 1 and 2. **B:** The relative locations of all mutations evaluated are indicated by colored arrows. Red arrows indicate locations of mutations in Prosper. Yellow and orange indicate locations of mutations in Kronos, with yellow denoting mutations that confer Ptr ToxB-insensitivity and the single orange mutation resulting in a sensitive reaction (i.e., no change from wild type). Black arrows indicate the physical positions of the two mutations shown in A along the gene structure.

Fig. 4: Genetic complementation by transformation of the wheat cultivar Fielder with the *TtExo70FX15* (*Tsc2*) gene.
A: Ptr ToxB infiltration of leaves of the durum cultivar Kronos, the common wheat cultivar Fielder, and Fielder transformed with the Kronos *Tsc2* (*TtExo70FX15)* gene, including ~2 kb upstream and ~2 kb downstream of the native start and stop codons (Fielder + *Tsc2*). **B:** Agarose gel electrophoresis of PCR-amplified fragments representing the 1.5 kb *TtExo70FX15* open reading frame in Kronos, Fielder, transgenic Fielder + *TtExo70FX15* (Fielder + *Tsc2*), and Gredho (Ptr ToxB insensitive and negative control) (lanes 1-12). The PCR experiments were done in triplicate. Lanes 13-16 show the PCR amplification of the endogenous *GAPDH* gene as a positive PCR control for each DNA sample. Source data are provided as a Source Data file.

Fig. 5: Transcriptional expression of *Tsc2*.
A: Transcriptional expression analysis of *Tsc2* in different wheat tissues using reverse transcription-PCR (RT-PCR). Amplification of the housekeeping gene *GAPDH* served as an endogenous control; the observed *GAPDH* amplicon corresponds to the expected cDNA product (187 bp), and no genomic DNA-derived product (357 bp) was detected. **B:** Temporal expression dynamics of *Tsc2* following infiltration with Ptr ToxB-producing culture and control yeast-peptone-dextrose (YPD) culture medium not producing Ptr ToxB in two-week-old Kronos seedlings. Quantitative real-time (qRT)-PCR was performed at 0, 6, 12, 24, 48, and 72 hours post-infiltration (hpi). Bars represent mean relative expression ± standard error of the mean (SEM); jittered dots represent individual biological replicates. Statistical differences between treatments were assessed by two-sided Welch's *t*-tests; exact *P*-values are shown above each comparison. Source data are provided as a Source Data file.

Fig. 6: Phylogenetics, structure, and localization of the Tsc2 protein.
A: Rooted maximum-likelihood (ML) phylogenetic tree of the Tsc2 protein relative to other Exo70FX proteins of the Poales, reconstructed from previously described datasets[40] by adding Exo70FX15 from *Aegilops* and *Triticum* species. Protein sequences were aligned using structure-guided multiple sequence alignment, and the tree was inferred using RAxML with a GAMMA model of rate heterogeneity. Red circles indicate bootstrap support greater than 80%. Branch lengths are proportional to the number of amino-acid substitutions per site; the scale bar indicates 0.1 substitutions per site. Bd = *Bracypodium distachyon*, Hv = *Hordeum vulgare* (barley), Ta = *Triticum aestivum* (common wheat), Ash = *Aegilops sharonensis*, Aes = *Aegilops speltoides*, Tt = *Triticum turgidum* ssp. *durum*, Tds = *Triticum turgidum* ssp. *dicoccoides*. **B:** Predicted 3D structure of the wheat TtExo70FX15 (Tsc2) protein compared to crystalized structures of yeast (ScExo70; PDB 2B1E) and Arabidopsis (AtExo70A1; PDB 4RL5) proteins, demonstrating the absence of the CorEX and CAT-A domains in TtExo70FX15 (Tsc2). **C:** Subcellular localization of TtExo70FX15 (Tsc2) and green fluorescent protein (GFP) control. Confocal microscopy images show fluorescence signals in the GFP channel (green), chlorophyll autofluorescence channel (red), bright-field channel, and merged images. Scale bar = 10 μm. Source data are provided as a Source Data file.

Fig. 7: Structures and phenotypes of the five DNA haplotypes and corresponding protein isoforms of *Tsc2* identified among 177 wheat accessions.
A: Haplotype structures and the reactions they confer to infiltrations with Ptr ToxB. Haplotype 1 encodes the canonical Ptr ToxB-sensitive isoform and differs from Haplotypes 2-5 by a 21-

nucleotide (nt) deletion. Haplotypes 2-5 share a 21-nt insertion encoding seven additional amino acids (WSLMVEP; highlighted in yellow). Haplotypes 3-5 harbor additional single-nucleotide substitutions (G1114C, A1331G, and G684A), indicated by orange bars and labeled above the haplotype schematic. Representative Ptr ToxB reactions of leaves for each isoform are shown to the right. **B:** The portion of superimposed predicted protein structures of Isoforms 1 and 2, encoded by Haplotypes 1 and 2, respectively, showing the structural consequence of the 21-nt indel. **C:** Protein cavity comparison in Isoform 1 vs Isoform 2. The central cavity is highlighted in red. The 21-nt insertion in Isoform 2, corresponding to the additional seven amino acids (residues 370-376), is shown in yellow.

Fig. 8: Evolution of wheat and the proposed formation and spread of the *Tsc2* allele conferring sensitivity to Ptr ToxB (Haplotype 1). The figure denotes the accepted evolutionary scenario giving rise to domesticated durum and common wheat. Grey circles indicate Ptr ToxB-insensitive (sub)species, and yellow circles indicate Ptr ToxB-sensitive species harboring the allele with the 21-nt deletion shown as *Tsc2_H1* (haplotype that results in amino acid Isoform 1). The point where the deletion occurred is indicated by the lightning bolt. Grey circles with '*Tsc2*' in green are insensitive to Ptr ToxB but harbor alleles that give rise to Haplotypes 2-5, which all lack the 21-nt deletion.

Fig. 9: Marker-assisted and gene editing tools developed for *Tsc2* elimination to confer tan spot resistance in wheat.
A-B: The two-step marker assay process for identification of Ptr ToxB-sensitive alleles in wheat. **A:** Step #1 – Screening for the presence/absence of a *Tsc2* allele. Scatter plot of Global Durum Panel (GDP) lines genotyped with the fluorescence-based absent allele–specific amplification (FAASA) assay *fcp1066*. The fluorescence clusters separate lines with an absent allele of *Tsc2* (blue; *Tsc2*-) from lines having a *Tsc2* allele (green; *Tsc2*+). Non-template controls (NTC) are represented by black diamonds. **B:** Step #2 – Screening of the green cluster from Step 1, which consists of lines all harboring a *Tsc2* allele, but a mixture of sensitive and insensitive haplotypes. Scatter plot of Global Durum Panel (GDP) lines genotyped with FAASA assay *fcp1077*, which discriminates the 21-nucleotide (nt) indel in *Tsc2.* Clusters distinguish the deletion allele (-21 nt; sensitive; blue) from the ancestral allele (+21 nt; insensitive; green). **C:** Gene-editing route to eliminate sensitivity. CRISPR/Cas9-mediated editing of *Tsc2* showing insertion of a cytosine after base position 39 (g.39_40insC), which induces a frameshift and introduces a premature stop codon. The sequence representation shows the predicted amino acids before and after the insertion: single letters correspond to the shared wild-type sequence upstream of the edit site, while stacked letters represent the divergence beyond the insertion point, with the upper row indicating the wild-type sequence and the lower row the CRISPR-induced mutant sequence that terminates prematurely. Leaf phenotype images on the right show Ptr ToxB sensitivity in wild type Kronos (Kronos-WT) versus Ptr ToxB insensitivity in the *tsc2* mutant, confirming the functional disruption of *Tsc2*.

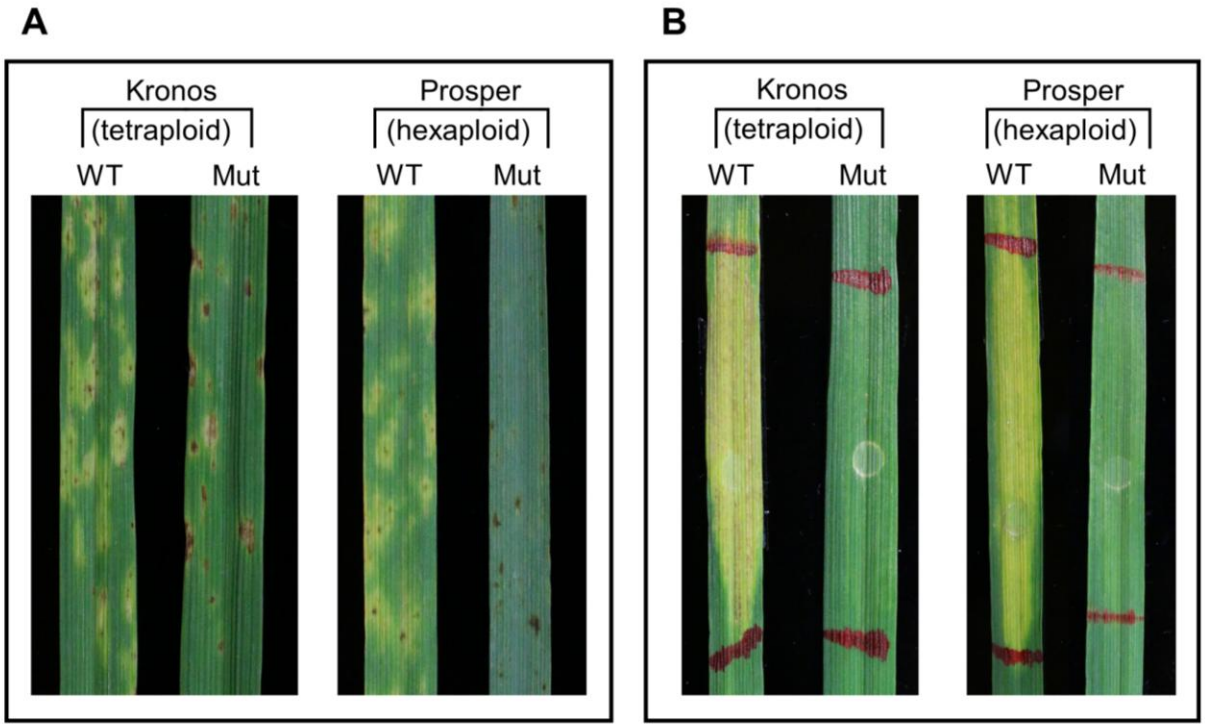


Fig. 1: Phenotypic effects of a compatible *Tsc2*-Ptr ToxB interaction in tetraploid (durum) and hexaploid (common) wheat.
A: Spray inoculation with the Ptr ToxB-producing *Pyrenophora tritici-repentis* race 5 isolate DW5. Wild-type durum wheat cultivar Kronos (tetraploid) and common wheat cultivar Prosper (hexaploid), which carry a functional *Tsc2* allele, exhibit expanding and coalescing chlorotic lesions in response to infection, whereas their corresponding *Tsc2*-disrupted mutants (Kronos2704 and Prosper89a) show infection site lesions with little to no chlorosis development or expansion. **B:** Leaf infiltration of cultures containing the necrotrophic effector Ptr ToxB. Wild-type Kronos and Prosper develop localized cell death at infiltration sites, whereas the *Tsc2*-disrupted mutants undergo no cell death. WT = wild type; Mut = *Tsc2*-disrupted mutant.

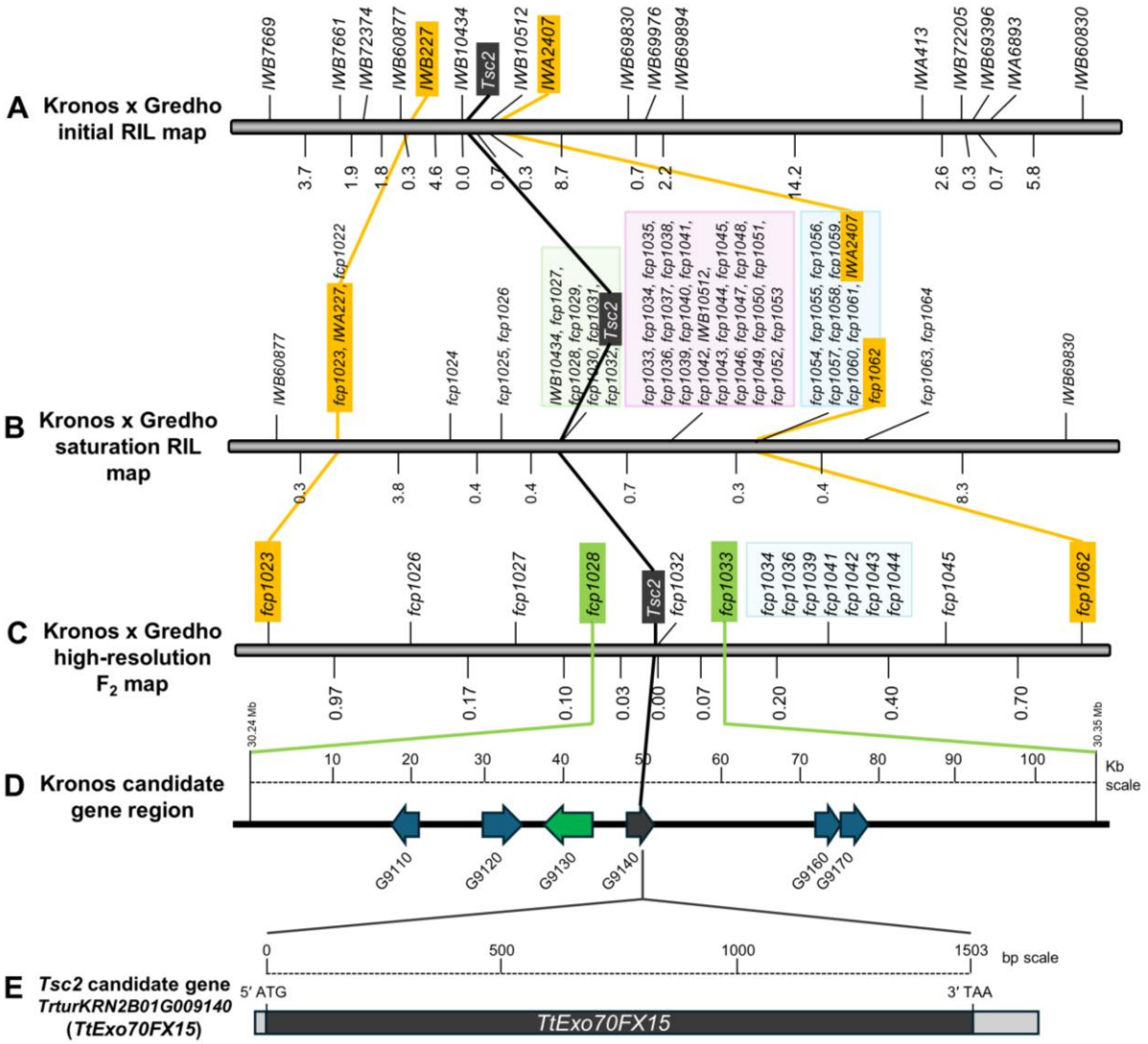


Fig. 2: Mapping and identification of candidate genes for *Tsc2*.
A: The initial genetic linkage map of the *Tsc2* region of chromosome arm 2BS generated in the Kronos × Gredho recombinant inbred population. The flanking markers used to define the target interval for marker development are highlighted in yellow. **B:** Saturated linkage map developed in the Kronos × Gredho recombinant inbred population by developing 43 additional markers. **C:** High-resolution linkage map developed in the Kronos × Gredho F_2 population between markers *fcp1023* and *fcp1062*. Along the genetic maps of A, B, and C, marker names are shown above the grey bars, and genetic distances in centimorgan (cM) are shown below. **D:** Physical map of the 108.4 kb candidate interval between markers *fcp1028* and *fcp1033* in the Kronos genome. Blue arrows represent conserved gene models shared between Ptr ToxB-sensitive and -insensitive lines, the green arrow indicates the leucine-rich repeat receptor-like kinase (LRR-RLK; *TrturKRN2B01G009130*), and the dark grey arrow represents the Exo70 family gene subsequently identified as *Tsc2* (*TtExo70FX15*; *TrturKRN2B01G009140*). **E:** The structure of candidate gene *TrturKRN2B01G009140* (*TtExo70FX15*), which consists of a single exon (dark grey). The untranslated regions are indicated by light grey shaded boxes.

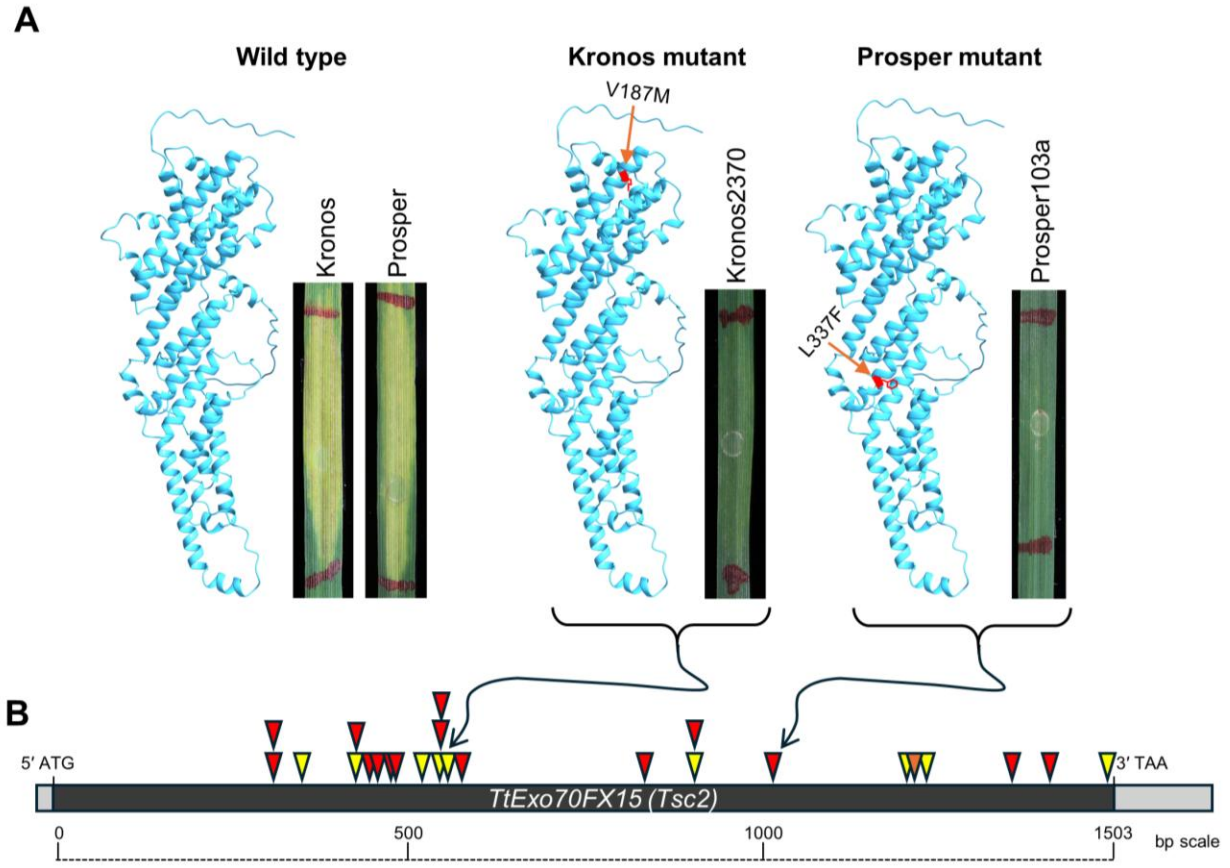


Fig. 3: Evaluation and analysis of mutations in the *TtExo70FX15* (*Tsc2*) gene in Kronos and Prosper.

A: Ptr ToxB infiltration reactions and predicted TtExo70FX15 (Tsc2) protein structures of the wild-type wheat lines Kronos and Prosper, and one representative missense mutant in each of the two lines that result in an insensitive reaction to Ptr ToxB. Protein structures depict the AlphaFold-predicted wild-type TtExo70FX15 (Tsc2) protein, with missense mutation sites highlighted to indicate their spatial positions within the structure. The locations of the point mutations in the two mutant proteins are indicated in red and indicated by orange arrows. Infiltration reactions and predicted protein structures for all other Kronos and Prosper *TtExo70FX15* (*Tsc2*) missense mutants are presented in Supplementary Figures 1 and 2. **B:** The relative locations of all mutations evaluated are indicated by colored arrows. Red arrows indicate locations of mutations in Prosper. Yellow and orange indicate locations of mutations in Kronos, with yellow denoting mutations that confer Ptr ToxB-insensitivity and the single orange mutation resulting in a sensitive reaction (i.e., no change from wild type). Black arrows indicate the physical positions of the two mutations shown in A along the gene structure.

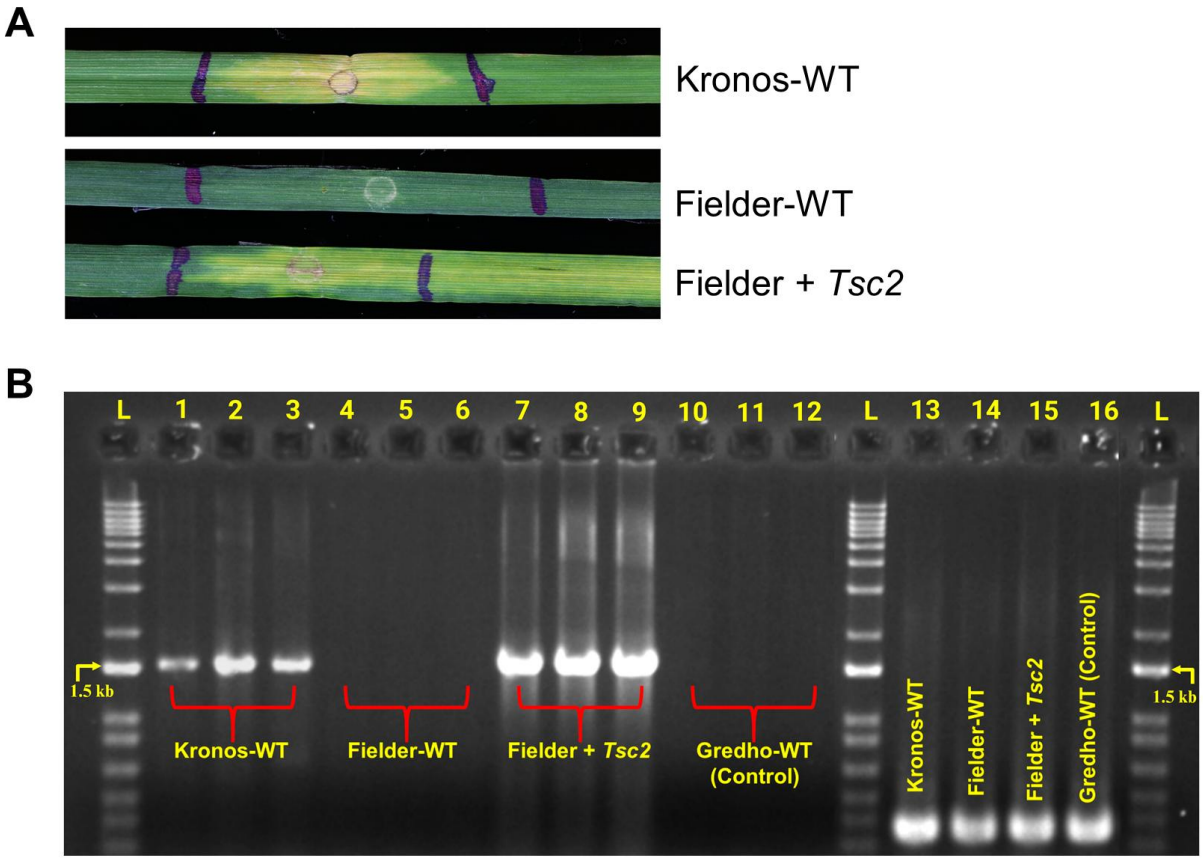


Fig. 4: Genetic complementation by transformation of the wheat cultivar Fielder with the *TtExo70FX15* (*Tsc2*) gene.
A: Ptr ToxB infiltration of leaves of the durum cultivar Kronos, the common wheat cultivar Fielder, and Fielder transformed with the Kronos *Tsc2* (*TtExo70FX15)* gene, including ~2 kb upstream and ~2 kb downstream of the native start and stop codons (Fielder + *Tsc2*). **B:** Agarose gel electrophoresis of PCR-amplified fragments representing the 1.5 kb *TtExo70FX15* open reading frame in Kronos, Fielder, transgenic Fielder + *TtExo70FX15* (Fielder + *Tsc2*), and Gredho (Ptr ToxB insensitive and negative control) (lanes 1-12). The PCR experiments were done in triplicate. Lanes 13-16 show the PCR amplification of the endogenous *GAPDH* gene as a positive PCR control for each DNA sample. Source data are provided as a Source Data file.

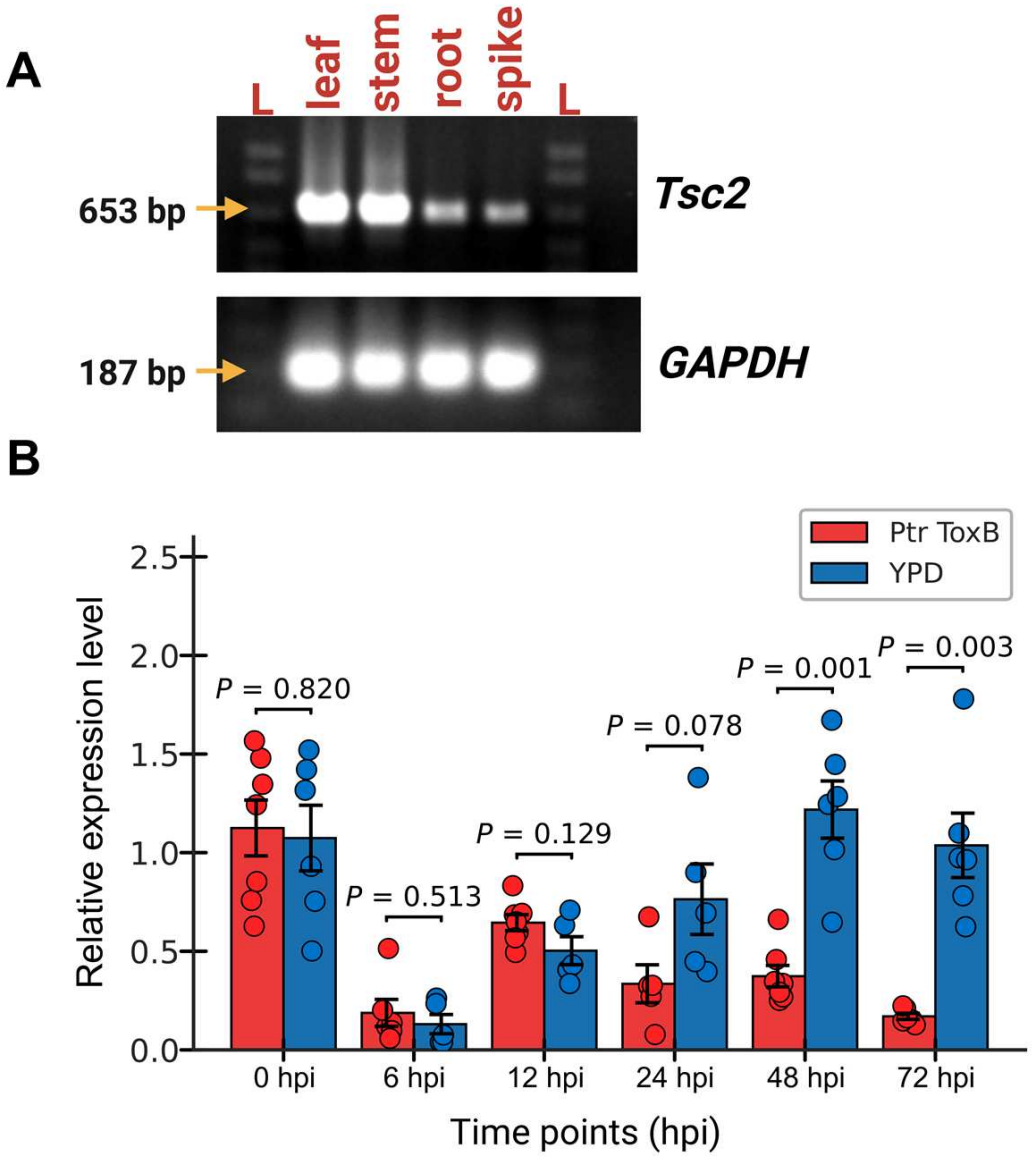


Fig. 5: Transcriptional expression of *Tsc2*.
A: Transcriptional expression analysis of *Tsc2* in different wheat tissues using reverse transcription-PCR (RT-PCR). Amplification of the housekeeping gene *GAPDH* served as an endogenous control; the observed *GAPDH* amplicon corresponds to the expected cDNA product (187 bp), and no genomic DNA-derived product (357 bp) was detected. **B:** Temporal expression dynamics of *Tsc2* following infiltration with Ptr ToxB-producing culture and control yeast-peptone-dextrose (YPD) culture medium not producing Ptr ToxB in two-week-old Kronos seedlings. Quantitative real-time (qRT)-PCR was performed at 0, 6, 12, 24, 48, and 72 hours post-infiltration (hpi). Bars represent mean relative expression ± standard error of the mean (SEM); jittered dots represent individual biological replicates. Statistical differences between treatments were assessed by two-sided Welch's *t*-tests; exact *P*-values are shown above each comparison. Source data are provided as a Source Data file.

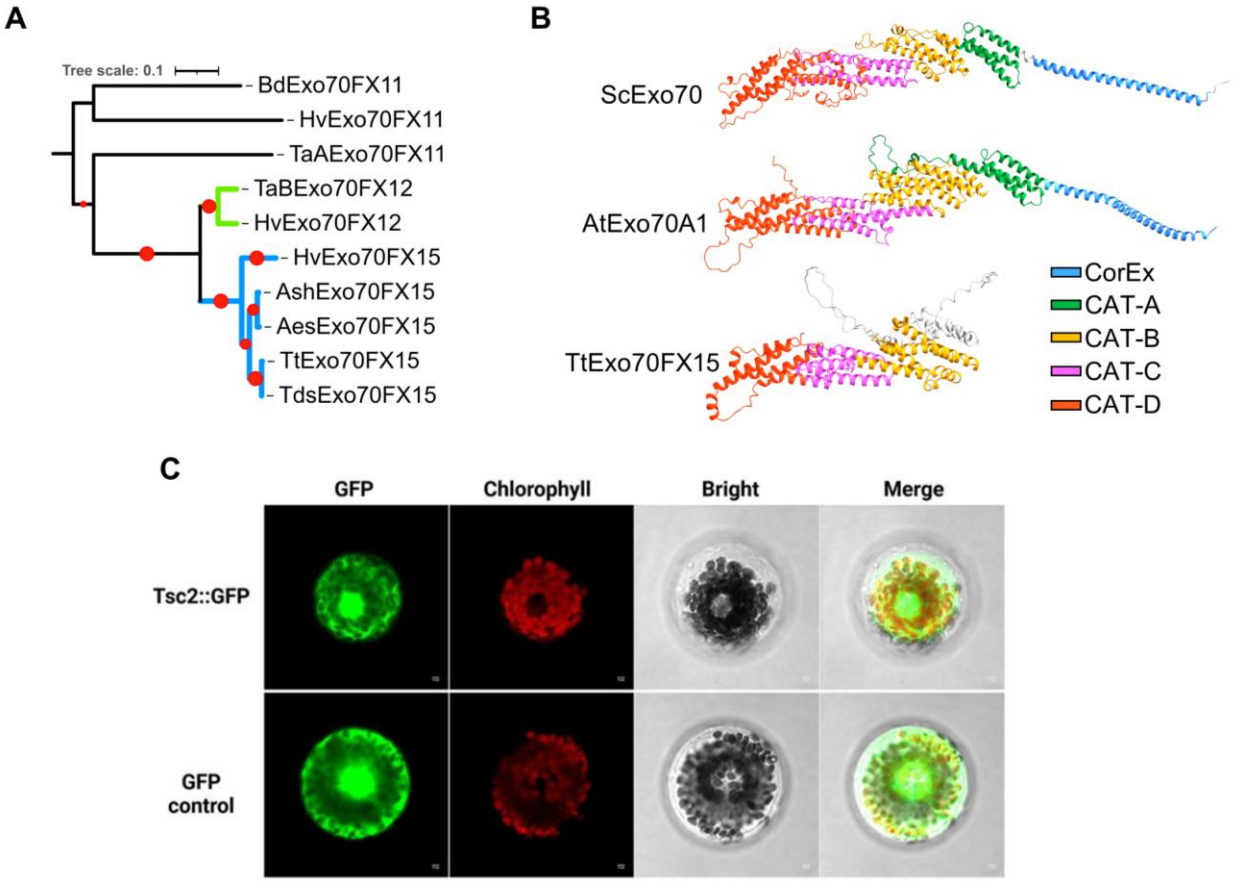


Fig. 6: Phylogenetics, structure, and localization of the Tsc2 protein.
A: Rooted maximum-likelihood (ML) phylogenetic tree of the Tsc2 protein relative to other Exo70FX proteins of the Poales, reconstructed from previously described datasets[40] by adding Exo70FX15 from *Aegilops* and *Triticum* species. Protein sequences were aligned using structure-guided multiple sequence alignment, and the tree was inferred using RAxML with a GAMMA model of rate heterogeneity. Red circles indicate bootstrap support greater than 80%. Branch lengths are proportional to the number of amino-acid substitutions per site; the scale bar indicates 0.1 substitutions per site. Bd = *Bracypodium distachyon*, Hv = *Hordeum vulgare* (barley), Ta = *Triticum aestivum* (common wheat), Ash = *Aegilops sharonensis*, Aes = *Aegilops speltoides*, Tt = *Triticum turgidum* ssp. *durum*, Tds = *Triticum turgidum* ssp. *dicoccoides*. **B:** Predicted 3D structure of the wheat TtExo70FX15 (Tsc2) protein compared to crystalized structures of yeast (ScExo70; PDB 2B1E) and Arabidopsis (AtExo70A1; PDB 4RL5) proteins, demonstrating the absence of the CorEX and CAT-A domains in TtExo70FX15 (Tsc2). **C:** Subcellular localization of TtExo70FX15 (Tsc2) and green fluorescent protein (GFP) control. Confocal microscopy images show fluorescence signals in the GFP channel (green), chlorophyll autofluorescence channel (red), bright-field channel, and merged images. Scale bar = 10 µm. Source data are provided as a Source Data file.

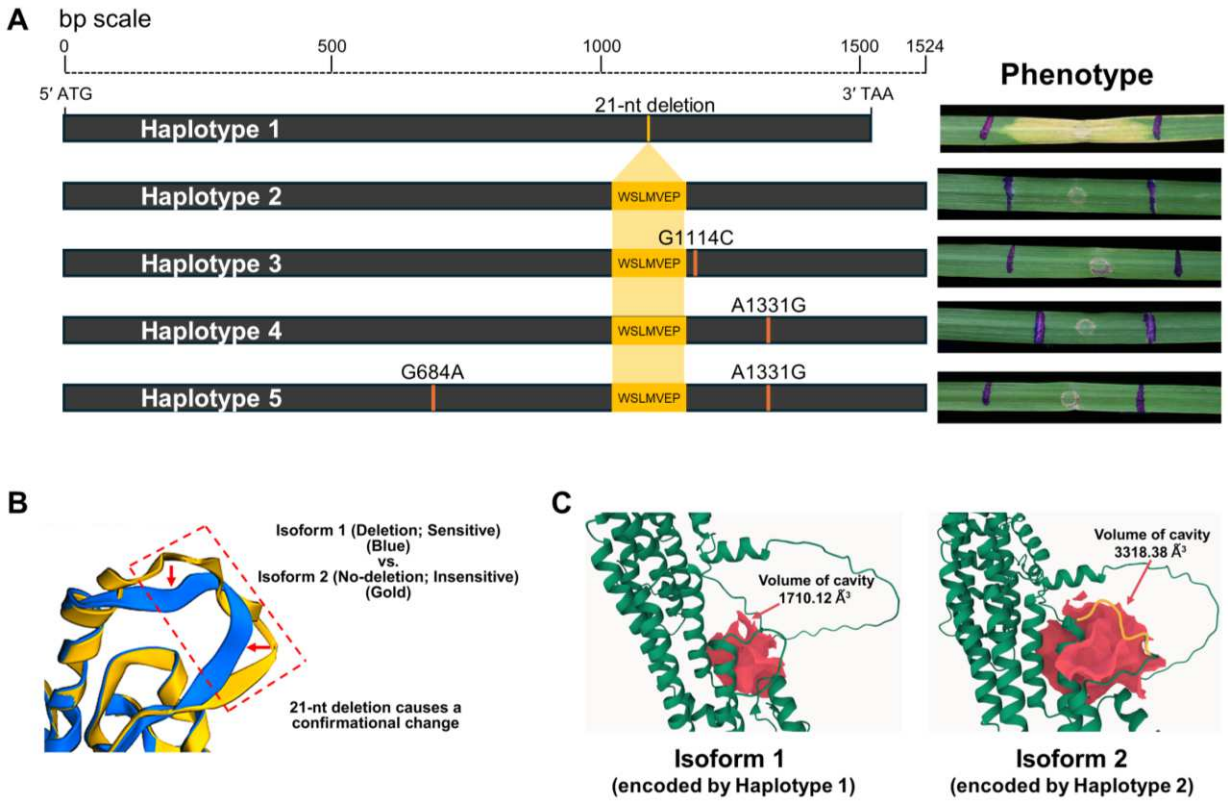


Fig. 7: Structures and phenotypes of the five DNA haplotypes and corresponding protein isoforms of *Tsc2* identified among 177 wheat accessions.
A: Haplotype structures and the reactions they confer to infiltrations with Ptr ToxB. Haplotype 1 encodes the canonical Ptr ToxB-sensitive isoform and differs from Haplotypes 2-5 by a 21-nucleotide (nt) deletion. Haplotypes 2-5 share a 21-nt insertion encoding seven additional amino acids (WSLMVEP; highlighted in yellow). Haplotypes 3-5 harbor additional single-nucleotide substitutions (G1114C, A1331G, and G684A), indicated by orange bars and labeled above the haplotype schematic. Representative Ptr ToxB reactions of leaves for each isoform are shown to the right. **B:** The portion of superimposed predicted protein structures of Isoforms 1 and 2, encoded by Haplotypes 1 and 2, respectively, showing the structural consequence of the 21-nt indel. **C:** Protein cavity comparison in Isoform 1 vs Isoform 2. The central cavity is highlighted in red. The 21-nt insertion in Isoform 2, corresponding to the additional seven amino acids (residues 370-376), is shown in yellow.

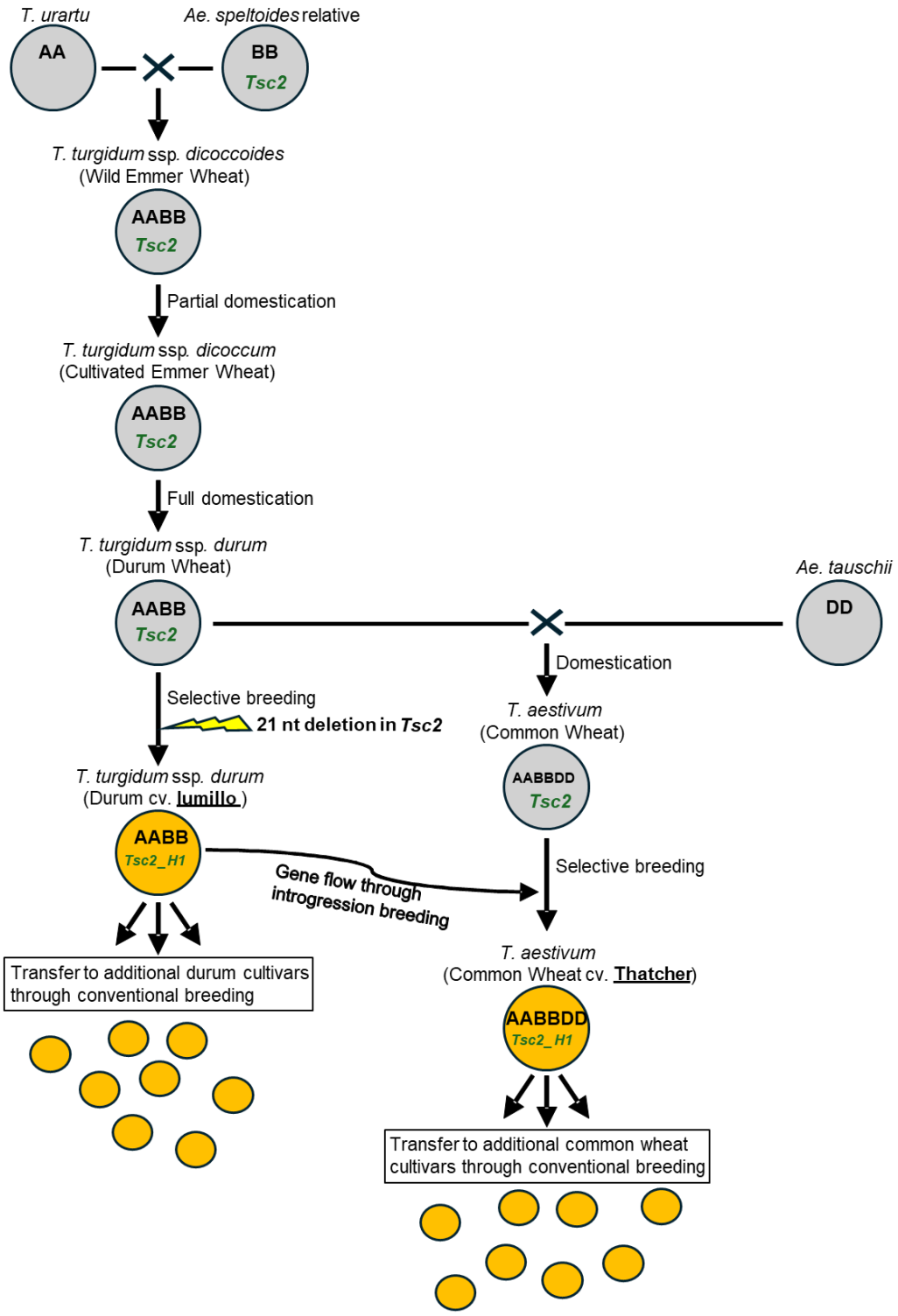


Fig. 8: Evolution of wheat and the proposed formation and spread of the *Tsc2* allele conferring sensitivity to Ptr ToxB (Haplotype 1). The figure denotes the accepted evolutionary scenario giving rise to domesticated durum and common wheat. Grey circles indicate Ptr ToxB-

insensitive (sub)species, and yellow circles indicate Ptr ToxB-sensitive species harboring the allele with the 21-nt deletion shown as *Tsc2_H1* (haplotype that results in amino acid Isoform 1). The point where the deletion occurred is indicated by the lightning bolt. Grey circles with '*Tsc2*' in green are insensitive to Ptr ToxB but harbor alleles that give rise to Haplotypes 2-5, which all lack the 21-nt deletion.

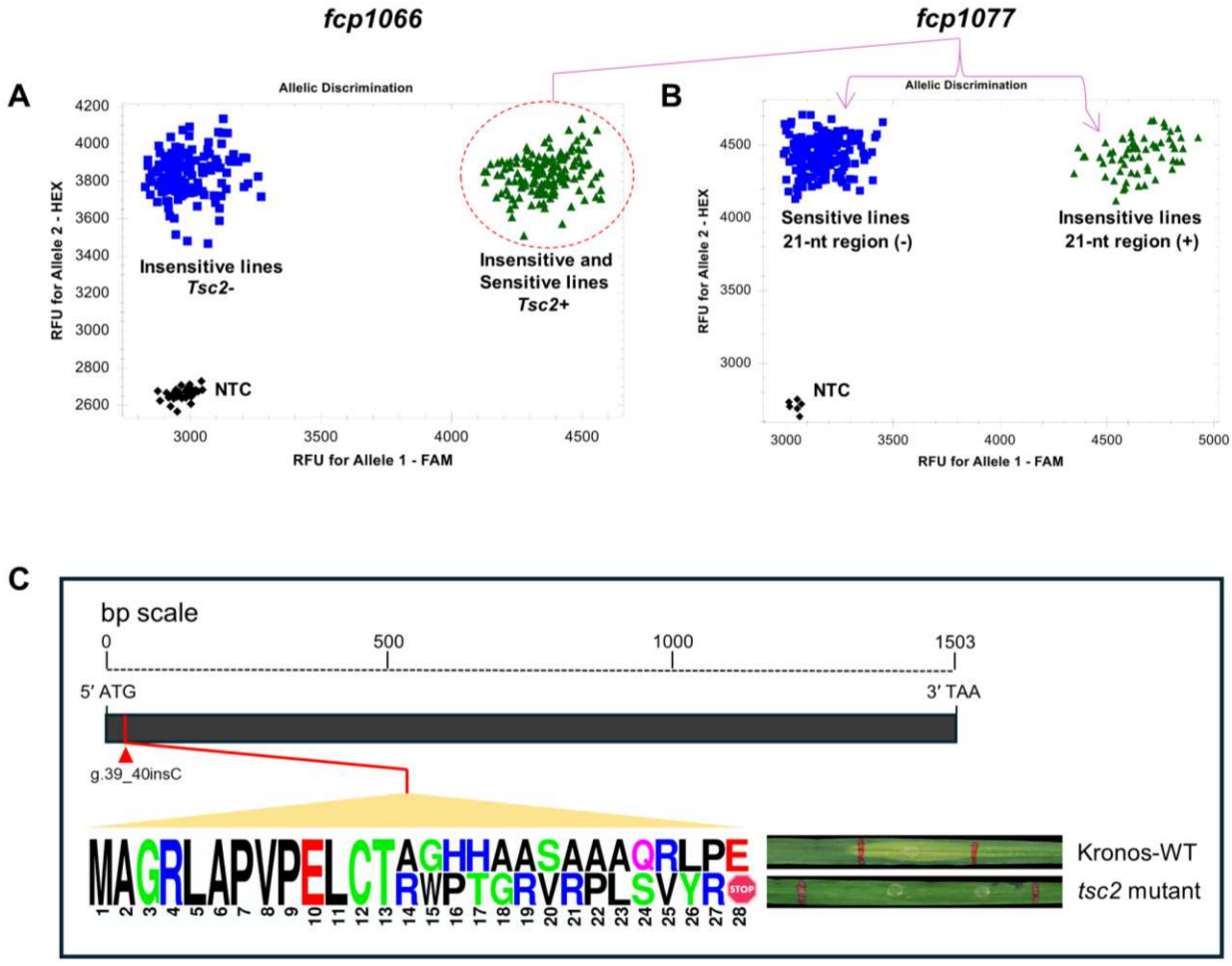


Fig. 9: Marker-assisted and gene editing tools developed for *Tsc2* elimination to confer tan spot resistance in wheat.

A-B: The two-step marker assay process for identification of Ptr ToxB-sensitive alleles in wheat. **A:** Step #1 – Screening for the presence/absence of a *Tsc2* allele. Scatter plot of Global Durum Panel (GDP) lines genotyped with the fluorescence-based absent allele–specific amplification (FAASA) assay *fcp1066*. The fluorescence clusters separate lines with an absent allele of *Tsc2* (blue; *Tsc2*-) from lines having a *Tsc2* allele (green; *Tsc2*+). Non-template controls (NTC) are represented by black diamonds. **B:** Step #2 – Screening of the green cluster from Step 1, which consists of lines all harboring a *Tsc2* allele, but a mixture of sensitive and insensitive haplotypes. Scatter plot of Global Durum Panel (GDP) lines genotyped with FAASA assay *fcp1077*, which discriminates the 21-nucleotide (nt) indel in *Tsc2.* Clusters distinguish the deletion allele (-21 nt; sensitive; blue) from the ancestral allele (+21 nt; insensitive; green). **C:** Gene-editing route to eliminate sensitivity. CRISPR/Cas9-mediated editing of *Tsc2* showing insertion of a cytosine after base position 39 (g.39_40insC), which induces a frameshift and introduces a premature stop codon. The sequence representation shows the predicted amino acids before and after the insertion: single letters correspond to the shared wild-type sequence upstream of the edit site, while stacked letters represent the divergence beyond the insertion point, with the upper row indicating the wild-type sequence and the lower row the CRISPR-induced mutant sequence that

terminates prematurely. Leaf phenotype images on the right show Ptr ToxB sensitivity in wild type Kronos (Kronos-WT) versus Ptr ToxB insensitivity in the *tsc2* mutant, confirming the functional disruption of *Tsc2*.

Supplementary Files

This is a list of supplementary files associated with this preprint. Click to download.

- SinghetalTsc2SupplementaryTables012726.xlsx
- SinghetalTsc2SupplementaryFigures012726.docx